**NATIONAL CENTER FOR EARTHQUAKE
ENGINEERING RESEARCH**

State University of New York at Buffalo

MULTIDIMENSIONAL MODELS OF HYSTERETIC MATERIAL BEHAVIOR FOR VIBRATION ANALYSIS OF SHAPE MEMORY ENERGY ABSORBING DEVICES

by

E. J. Graesser and F. A. Cozzarelli
Department of Civil Engineering
State University of New York at Buffalo
Buffalo, New York 14260

Technical Report NCEER-89-0018

June 7, 1989

NOTICE

MULTIDIMENSIONAL MODELS OF HYSTERETIC MATERIAL BEHAVIOR FOR VIBRATION ANALYSIS OF SHAPE MEMORY ENERGY ABSORBING DEVICES

by

E.J. Graesser[1] and F.A. Cozzarelli[2]

June 7, 1989

Technical Report NCEER-89-0018

NCEER Contract Number 88-2010

NSF Master Contract Number ECE 86-07591

1   Research Assistant, Dept. of Mechanical Engineering, State University of New York at Buffalo
2   Professor, Dept. of Mechanical Engineering, State University of New York at Buffalo

NATIONAL CENTER FOR EARTHQUAKE ENGINEERING RESEARCH
State University of New York at Buffalo
Red Jacket Quadrangle, Buffalo, NY 14261

//

PREFACE

The National Center for Earthquake Engineering Research (NCEER) is devoted to the expansion and dissemination of knowledge about earthquakes, the improvement of earthquake-resistant design, and the implementation of seismic hazard mitigation procedures to minimize loss of lives and property. The emphasis is on structures and lifelines that are found in zones of moderate to high seismicity throughout the United States.

NCEER's research is being carried out in an integrated and coordinated manner following a structured program. The current research program comprises four main areas:

- Existing and New Structures
- Secondary and Protective Systems
- Lifeline Systems
- Disaster Research and Planning

This technical report pertains to Program 2, Secondary and Protective Systems, and more specifically, to protective systems. Protective Systems are devices or systems which, when incorporated into a structure, help to improve the structure's ability to withstand seismic or other environmental loads. These systems can be passive, such as base isolators or viscoelastic dampers; or active, such as active tendons or active mass dampers; or combined passive-active systems.

Passive protective systems constitute one of the important areas of research. Current research activities, as shown schematically in the figure below, include the following:

1. Compilation and evaluation of available data.
2. Development of comprehensive analytical models.
3. Development of performance criteria and standardized testing procedures.
4. Development of simplified, code-type methods for analysis and design.
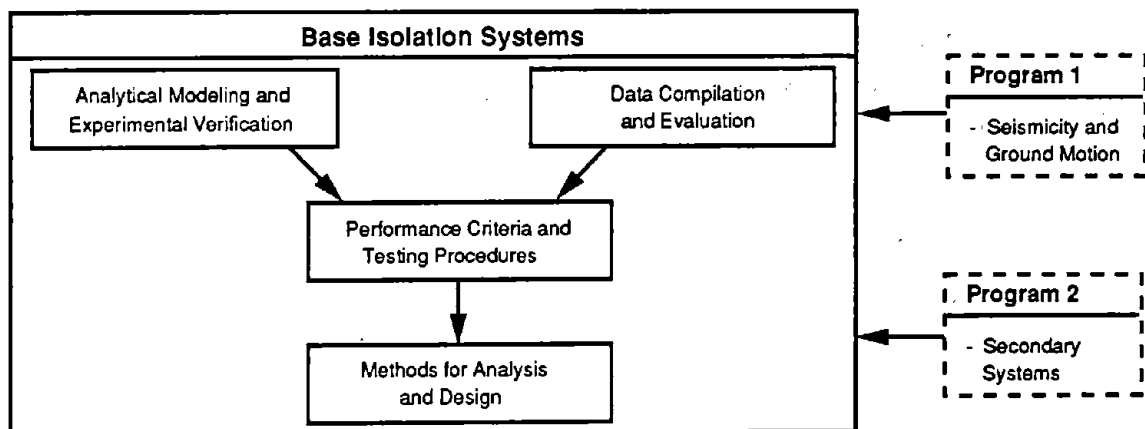
The Center provided funding to the State University of New York at Buffalo to conduct a program of analytical and experimental research on the possible use of shape memory materials in passive protective systems for building structures. This report presents the results of the analytical research that has been carried out at SUNY/Buffalo. The following sections detail the analytical models used, results obtained, and conclusions that can be drawn from this investigation.

ABSTRACT

Ozdemir's model of one-dimensional hysteretic force-deformation behavior for base isolation energy absorbing devices is selected as a basis for more general models of material point stress-strain behavior. The modification of the backstress allows for the description of material behavior associated with shape memory materials. The shape memory material behavior characteristics are of interest for base isolation and structural bracing technologies due to their high damping capacity. The one-dimensional models of metal plasticity and shape memory material behavior are extended to three-dimensional tensor representations which involve deviator expressions and their associated invariants. The resulting formulations for the one-dimensional case are used in calculations for the cyclic stress-strain behavior of both models. The resulting hysteretic data show the convenient aspects of both models for one-dimensional analytical studies.

Preceding page blank

LIST OF ILLUSTRATIONS

Preceding page blank

SECTION I

INTRODUCTION

In the event of an earthquake it is now possible to achieve reductions in the structural vibratory response and associated structural damage of buildings by utilizing passive control measures and incorporating them into building design. Base isolation is one modern means of passively controlling structural vibration and it is a technology which is being studied with continually increasing interest. The concept of base isolation has been demonstrated as viable both in the laboratory and in practice. An excellent overview of the history, development, and modern state of base isolation technology is presented in a review by Kelly [1]. Many specific studies have been made on elastomeric, lead-rubber, and frictional base isolation devices. The success of these studies has ultimately led to implementation of base isolation technology in a variety of worldwide locations.

Another means of mitigating seismic structural vibration is available through the installation of energy absorbing devices in the structure of a building. A study involving the implementation of viscoelastic energy absorbing devices for increased structural damping has been carried out at NCEER [2]. In the study, this structural damping concept was analyzed experimentally by adding the viscoelastic dampers to a model structure as bracing members and then testing the model structure on the NCEER seismic simulator. Results from this study show that overall structural performance under seismic conditions can be improved with added viscoelastic dampers. Also evident from the study is the existence of a temperature dependence which strongly influences the efficiency of the viscoelastic dampers. This result is not surprising due to the well known sensitivity of viscoelastic material properties to temperature.

Since the applied technologies associated with the base isolation concept and the concept of added viscoelastic dampers are relatively new, little has been done to investigate the use of other damping materials for these fields. Consider for a moment some of the properties which a candidate material should exhibit for possible use in base isolation. The overall material behavior should ideally exhibit a significant hysteretic (or energy absorbing) effect without sacrificing stiffness at low strains. Furthermore, it is also desirable that the damping properties of the device be optimum for the increased levels of strain and strain rate which occur during strong earthquake activity. Also, in the event of extreme ground displacements it is desirable to achieve increased stiffness at very large levels of strain. In order to explore these phenomena, a material model should be developed and employed which is general enough to include a variety of different types of inelastic material behavior. In addition, it is desirable that such a material model be closely linked to experimental studies of properties for a broad range of materials.

One potentially useful class of materials being considered in the present research are shape memory alloys (SMA's). The SMA's are a class of metals which are characterized by the so called "shape memory effect" that results from a first order martensitic phase transition. This micromechanical phase transition process is capable of producing a high damping capacity in SMA's as compared to conventional metals [3]. Refer for a moment to Figure 1-1. In this figure the basic forms of SMA behavior are shown. Figure 1-1a shows SMA behavior at ampient temperatures T < M_f. M_f is the temperature wherein the microstructure is fully martensitic. This stress-strain behavior is characterized by a large hysteresis loop similar to that exhibited by conventional steels. However, the hysteresis which results from cyclic loading is not due to dislocation glide (as in most metals). Rather, the

hysteresis is due to deformation of martensite which occurs by rotation, growth, and shrinkage of individual variants of martensite (of which there are 24). These variants form a single parent grain. If strained sufficiently only one variant will remain. This variant reverts uniquely to the original parent crystal orientation upon the application of heat, thus the memory effect.

Figure 1-1b shows the behavior of the SMA at temperature $T > A_f$ and shows the associated superelastic hystereis loop which ideally provides a hysteretic effect and has zero residual strain upon unloading. Note that A_f is the temperature above which the microstructure is fully austenitic. This superelastic SMA behavior results from the elastic loading of a stable austenitic parent phase up to a threshold stress whereupon a stress induced transformation from austenite to martensite takes place. This transformation process occurs at a significantly reduced modulus thus giving the appearance of a yield point. As deformation proceeds the volume of martensite within the microstructure increases and the path of the stress-strain curve follows a stress plateau. As the microstructure becomes fully martensitic, further straining will cause the martensite to be loaded elastically at a modulus lower than that of elastic austenite but much higher than that of the phase transition portion of the loading curve. Since the martensite is stable only due to the presence of the applied stress, a reverse transformation takes place upon unloading, but at a lowered stress plateau. Ideally, after full unloading, the material returns to its original undeformed geometry. This remarkable process yields the hysteretic effect with zero residual strain and thus motivates the asaciated term of superelasticity. High temperature applications of SMA's display linear elastic behavior with no hysteresis as shown schematically in Figure 1-1c.
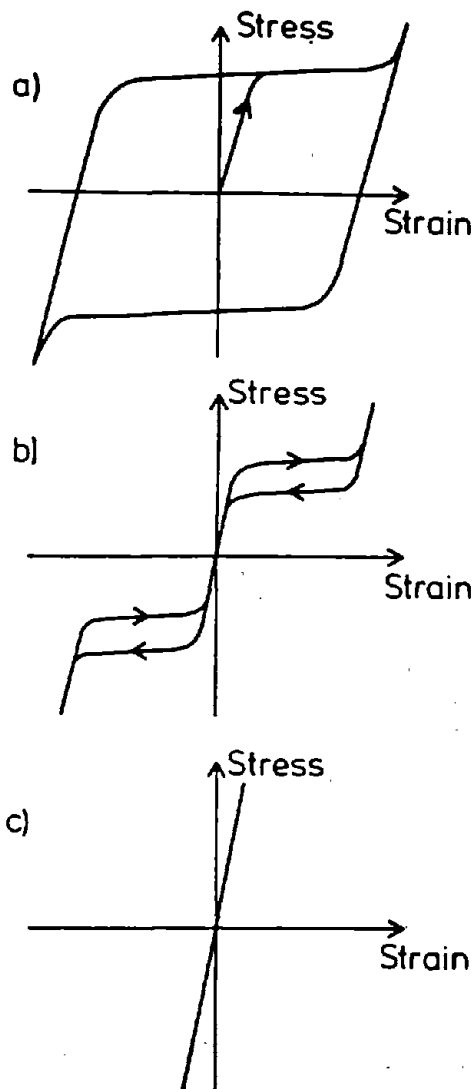
Figure 1-1 Schematic Stress-Strain Curve of Shape Memory Alloys (SMA's) [4]

    (a)   at temperature $T < M_f$: Large Area Hysteresis

    (b)   at temperature $T > A_f$: superelasticity

    (c)   at high temperature: elasticity

Thus, the modes of material response which are of interest in this research are given by Figure 1(a) (SMA hysteresis) and Figure 1(b) (superelastic). Some promising characteristics of these two modes of SMA behavior include high stiffness for small strain levels (elastic loading), reduced stiffness for intermediate levels of strain (due to formation and/or reorientation of martensite), and high stiffness at large levels of strain (elastic loading of martensite). Also, since the superelastic material ideally displays a hysteretic effect with zero residual strain, an energy absorbing isolation device made from this material would theoretically provide a centering force for the building following a seismic event.

Another interesting metallurgical aspect of the shape memory alloy is its capacity to display a variation in its hysteretic behavior which can be controlled by the selection of the material composition and various heat treatments applied to the material [5]. The heat treatment ultimately determines the extent of martensitic phase transformation in the superelastic material and this is the primary factor which allows for variation of the observed hysteretic behavior in these materials. Once the heat treatment has been applied, the subsequent material behavior is essentially insensitive to normal environmental temperature changes experienced in building design. Thus, the SMA may also be a potentially functional candidate for use in the design of structural damping devices due to its potentially large damping capacity as well as its insensitivity to environmental temperature changes.

These are the basic premises which give foundation to the undertaken research. In the discussion of the following sections the aspect of material modeling is carefully reviewed, developed, and presented and is done so in a way that is pertinent to the field of secondary and protective systems in earthquake engineering.

SECTION 2

SURVEY OF HYSTERETIC MODELS

2.1 Background

Based on the nature of this research, a model of inelastic material behavior is required for the analysis of base isolation devices and structural damping devices. This need arises from the hysteretic behavior that is induced in these energy absorbing devices during seismic activity. The hysteretic behavior observed in the energy absorbing devices is markedly different from the observed vibrational behavior in the structural framing members of buildings. Energy absorbing devices may typically experience repeated deformation excursions well into the inelastic range whereas the deformation encountered in steel framing members and structural joints is either elasitic or locally plastic.

The development of the base isolation concept and its evolution up to the present time is discussed in the review paper of Kelly [1]. In this paper a large bibliography is given which includes references for the design characteristics of existing base isolation devices as well as references for experimental and computational analyses of base isolated structures. In many computational studies, hysteretic models are used to represent the base isolation device. Such studies provide a starting point for this research. A primary requirement for any material model which is to be used in analysis is that it reproduce experimentally observed hysteretic behavior to a reasonable degree of accuracy. Also desirable in the model is a physically motivated basis in the governing formulation of equations. This allows for studies involving variation of the material characteristics which give reasonably approximate predictions of the response without recourse to experiment. This may be especially useful when considering the various types of attainable behavior in the shape memory materials.

2-1

2.2 Models of Hysteretic Behavior

A survey of literature from the field of base isolation indicated a popular use of the hysteretic model of Wen [6]. In Wen's paper, a method for general random hysteretic system response is presented. The hysteretic model given in [6] is often used to represent the hysteretic behavior of a fully characterized base isolation device in random structural vibration studies (such as in [7]). In a similar structural analysis incorporation of a slip-lock element with Wen's model allowed for simulated hysteresis loop pinching behavior [8]. Thus Wen's model is attractive for structural studies especially pertaining to a seismic base isolation. However, a drawback of Wen's model for the purposes of this research is its lack of physically motivated expressions in the governing formulation. As such, Wen's model is empirically rather than physically motivated. It is often difficult to interpret the parameters of an empirical model and associate them with the physical parameters of the real material or device. Thus, other models which possess a more physically motivated formulation are also considered.

In a hysteresis model from Iwan [9] the hysteretic system is considered to be a parallel distribution of ideal Elastoplastic elements having varying yield levels. This arrangement is shown in Figure 2-1. The model of Figure 2-1 can then be related back to a material or device by making a physical analogy. For example, the parallel distribution of elastoplastic elements can be thought of as analogous to a slip plane in a solid material or as analogous to a slip joint or yielding member in some more complicated device. In [9] the author demonstrates how the distributed element formulation can be used to generate a relatively simple hysteretic model which is capable of exhibiting the essential features of one dimensional dynamic hysteretic systems. This model, while attractive due to its physical motivation, is somewhat oversimplified for the undertaken research.

2-2
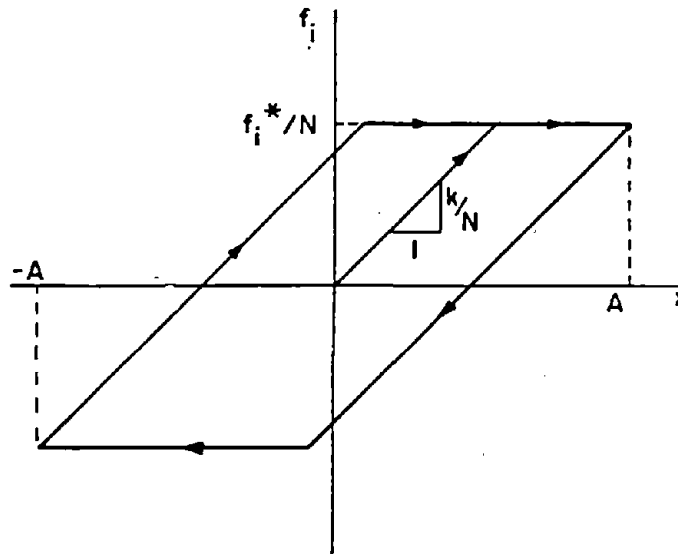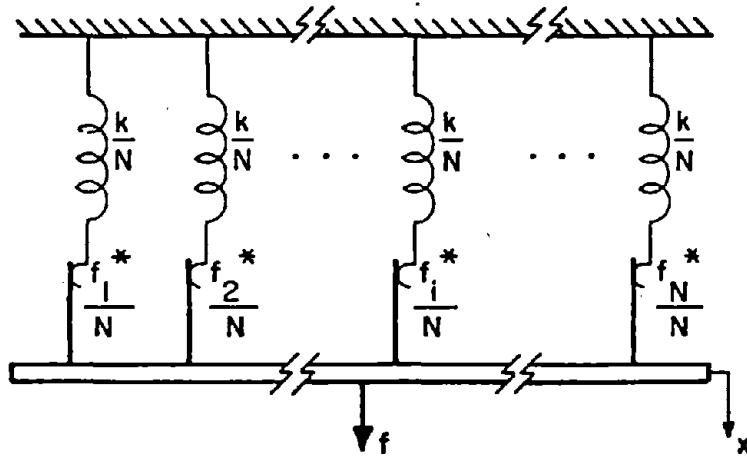
Figure 2-1 Model Consisting of a Distribution of Elastoplastic Elements [9]

2.3 Models of Viscoplasticity

There also exists a fairly large selection of material models in the area of viscoplasticity. Many current researchers in this field take an approach which unifies the constitutive laws of creep and plasticity based on the fact that the primary mechanism in almost all creep and plasticity processes is the motion of dislocations in the microstructure. The models of the unified approach are described by a constitutive differential equation and an associated set of internal variables. The internal variables are usually described by separate growth laws which involve various physical parameters of the material, and as such can be used to physically model material behavior. Also, these unified models are often written in terms of tensor quantities thus permitting multiaxial formulations and analysis. A recent text edited by Miller [10] gives six separate models of the unified approach from prominent researchers in the field. Also, a review article by Krempel [11] cites the history, development, and modern methods of viscoplastic modeling including selected models of the unified approach. A dissertation reflecting Krempel's philosophy is written by Yao [12] and gives a viscoplasticity model based on overstress. This model is also in tensor form and is given from the same perspective as other theories of the unified approach. These models, although accurate, may be somewhat complex for the nature of the research ongoing in this project.

2.4 Ozdemir's Model

The most desirable model for the purposes of this research is one which accurately reproduces the hysteretic behavior of damping materials or devices while retaining a relatively simple form and physically motivated expressions. One such model which may meet these requirements is given in a dissertation written by Ozdemir [13] under the supervision of Kelly. In Ozdemir's work a one dimensional nonlinear transient dynamic model is

presented for yielding structures. The model was developed and verified for aseismic base isolation studies and as such is useful for the ongoing research in this project. The model in [13] essentially expresses the strain rate as a sum of elastic and inelastic components as is usually done in most strain rate expressions [14, 5, 11, 12]. The inelastic component is a function of the overstress and as such is similar to other unified theories such as in [11] and [12]. Also, the model of interest from [13] appears to be tractable to an extension from a one dimensional expression to a three dimensional tensor representation. The approach for such an extension is given in Section 4.2 of this report.

2.5 Models of Shape Memory Alloy (SMA) Behavior

Since shape memory materials will be receiving a certain degree of attention in the present research, models developed to specifically predict their stress-strain behavior are also of interest. Some attempts have been made in this area, unfortunately however, at the present time there are very few models that predict the macroscopic SMA stress-strain behavior. In an article by Falk [4], a model of the shape memory effect is based on a free energy expression. The various mechanical and thermodynamic quantities are studied for crystal structures of austenite and martensite twins. The shear stress and shear strain relationship for the crystal is obtained based on a proposed Helmholtz free energy function. However, the stress-strain function in [4] is very simple and when tested numerically did not generate meaningful hysteresis loops.

Another more advanced model of shape memory behavior is proposed by Achenbach et. al. for memory alloys in plane strain [15]. The model is applicable to polycrystalline bodies under biaxial loading and also accounts for the rotational component of the deformation field. The deformation in SMA's is closely linked to phase fractions of austenite and martensite twins

and as such the model of [15] includes these phase fractions in the formulation as internal variables. The primary differential equation given in [15] to govern the material behavior of the SMA is analogous to the constitutive strain rate tensor equation of the flow type with internal variables used in unified theories of creep and plasticity. Thus the basic governing equations of the two fields are very similar. The full formulation of the SMA model of [15] is far to complex for practical use in the context of this research. However, its primary form suggests that the general constitutive form of the unified approach may also be applicable to SMA behavior by modifying the descriptions for the internal variables.

Therefore, the direction that has been taken thus far is one wherein a model of hysteretic behavior has been altered so as to allow for the basic material characteristics of the SMA to be displayed. The model by Ozdemir [13] has been found to be useful in this task. Also, in order to allow for possible multiaxial formulations, the single dimensional models of inelastic behavior and of SMA behavior have also been extended to three dimensional tensor representations.

HYSTERETIC MODEL FOR USE IN ANALYSIS

3.1 Introduction

When considering the various models available for hysteretic material behavior it is found that the model given in [13] has many features that render it useful for the endeavors of this research. This model was developed so that the force-deformation characteristics of base isolation energy absorbing devices could be predicted computationally. The differential equations presented in [13] specifically pertain to one dimensional nonlinear transient dynamic hysteretic behavior. One characteristic of many base isolation devices is that they are only slightly sensitive to the applied rate of deformation [13]. Such rate independence is a desirable trait under the varying conditions of loading encountered in seismic events, and it is shown in [13] that the use of rate independent equations to model hysteretic energy absorbing devices is the most effective means of accurately describing their behavior.

3.2 Force Deformation Equations in One-Dimension

The starting equations for this research will be a set of rate independent equations which describe the force deformation characteristics of hysteretic energy absorbing devices from [13]. For initial development and analysis any terms which allow for changing material characteristics (e.g. yield strength, modulus) or changing hardening characteristics will be left out of the ensuing equations. Thus the following equations, taken from [13], describe rate independent hysteretic behavior with non-deteriorating hardening characteristics and non-deteriorating material characteristics:

$$\frac{\dot{F}}{F_o} = \frac{\dot{U}}{U_o} - \left| \frac{\dot{U}}{U_o} \right| \left(\frac{F-S}{F_o} \right)^n \qquad (3.1)$$

$$\frac{\dot{S}}{F_o} = \alpha \left| \frac{\dot{U}}{U_o} \right| (\frac{F-S}{F_o})^n \qquad (3.2)$$

where

$F(t)$: represents the force in the hysteretic device.

$U(t)$: represents the displacement.

F_o : represents the yield force of the device.

U_o : represents the yield displacement of the device.

α : is a material constant which controls the slope of the F-U curve. Given approximately by $\alpha \approx K_y/(K_o - K_y)$ where $K_o = F_o/U_o$ and K_y is the slope of the F-U curve after yielding.

n : is a material constant which controls the sharpness of transition from the elastic to plastic state. An odd integer.

$(\dot{\ })$: ordinary differentiation with respect to time.

Note in Eqs. (3.1) and (3.2) that the function S is an internal force variable that is analogous to the backstress and the quantity (F-S) is analogous to the overstress (or effective stress), as used in many viscoplastic constitutive laws [10, 11, 12].

Eqs. (3.1) and (3.2) can be shown to give values of force and displacement which are independent of the applied rates of loading, i.e. not dependent on either of the rates $\dot{F}$ or $\dot{U}$. To show this, the case of positive displacement rate loading is used. By subtracting Eq. (3.2) from Eq. (3.1) the following differential equation is obtained

$$\frac{\dot{F}-\dot{S}}{F_o} = \frac{\dot{U}}{U_o} \left[1 - (1+\alpha) (\frac{F-S}{F_o})^n \right]$$

3-2

This result can be reexpressed as

$$d(\frac{U}{U_o}) = \frac{d(\frac{F-S}{F_o})}{1 - (1+\alpha) (\frac{F-S}{F_o})^n}$$

Then by integration the solution for the displacement can be shown to be

$$U = \frac{U_o}{(1+\alpha)^{1/n}} \int_o^{\frac{F-S}{F_o}} \frac{d\xi}{1-\xi^n}$$

It can easily be seen that the above integral is a function only of the difference F-S, i.e.

$$U = \phi(F-S)$$

By this process it becomes evident that Eqs. (3.1) and (3.2) represent rate independent Force-Displacement behavior.

3.3 Generalization to a Material Point Stress-Strain Relationship

Eqs. (3.1) and (3.2) are expressed with force and displacement as the primary variables. This is done because the studies undertaken in [13] concentrate on the overall behavior of the energy absorbing devices as a whole, including geometrical effects. It would have been impractical, for the studies in [13], to have used a set of constitutive equations which describe material behavior at a single point. However, for the research undertaken here, the reverse is true. Here, a characterization of the material behavior is first made with a set of constitutive relations and later

the material properties and behavior characteristics can be used for the design of an energy absorbing device. Therefore Eqs. (3.1) and (3.2) are now reexpressed, in an equivalent manner, in terms of stress and strain

$$\dot{\sigma} = E \left[\dot{\varepsilon} - |\dot{\varepsilon}|(\frac{\sigma-\beta}{Y})^n\right]$$ (3.3)

$$\dot{\beta} = \alpha E \, |\dot{\varepsilon}|(\frac{\sigma-\beta}{Y})^n$$ (3.4)

where

σ : is the one dimensional stress.

ε : is the one dimensional strain.

β : is the one dimensional back stress.

E : is the elastic modulus.

Y : is the yield strength.

α : is a constant controlling the slope of the $\sigma - \varepsilon$ curve. Given approximately by $\alpha \approx E_y/(E - E_y)$ where E_y is the slope of the $\sigma - \varepsilon$ curve after yielding.

n : is a constant controlling the sharpness of transition from elastic to plastic states.

$\dot{(\ )}$: ordinary time derivative.

By rearranging Eq (3) it follows that

$$\dot{\varepsilon} = \frac{\dot{\sigma}}{E} + |\dot{\varepsilon}| \, (\frac{\sigma-\beta}{Y})^n$$

Examination of this equation reveals that the total strain is made up of two separate components 1) a linear elastic component σ/E and 2) a

nonlinear inelastic component, ε^{in}, which is described by the rate expression $\dot{\varepsilon}^{in} = |\dot{\varepsilon}|[(\sigma - \beta)/Y]^n$. This inelastic component is a function of the total strain rate $\dot{\varepsilon}$ and the overstress $\sigma-\beta$. Later in this report these one dimensional equations for the $\sigma-\varepsilon$ hysteretic material behavior will be extended to a three dimensional tensor representation, and at that time it will be seen that the form of the extended equations will be similar to other models of viscoplastic behavior. In the meantime the one dimensional equations which are presently being considered are rewritten for clarity.

$$\dot{\varepsilon} = \frac{\dot{\sigma}}{E} + |\dot{\varepsilon}| \ (\frac{\sigma-\beta}{Y})^n \tag{3.5}$$

$$\dot{\beta} = \alpha E \ |\dot{\varepsilon}| \ (\frac{\sigma-\beta}{Y})^n \tag{3.6}$$

Thus Eqs. (3.5) and (3.6) describe the one dimensional hysteretic behavior of stress and strain for rate independent materials which undergo cyclic inelastic deformation.

3.4 Modification to Include SMA Behavior

Modifications of Eqs. (3.5) and (3.6) are also of interest since an altered set of equations may allow for a description of cyclic SMA hysteretic and/or superelastic behavior. The equation for the slope of the $\sigma-\varepsilon$ curve may lend some information to achieve this end. By returning to Eq. (3.5), rearranging back to the form of Eq. (3.3) and then dividing through by $\dot{\varepsilon}$, the equation for the slope of the $\sigma-\varepsilon$ curve is obtained

$$\frac{d\sigma}{d\varepsilon} = E \left[1 - \text{sgn}(\dot{\varepsilon}) \ (\frac{\sigma-\beta}{Y})^n\right]$$

By examining this expression one can see that the slope is constant during linear elastic loading and unloading (that is when the inelastic component of

strain is negligible). Also, it is possible to modify the shape of the inelastic portion of the σ-ε curve by altering the expression for the inelastic strain or by altering the expression defining the backstress β. Trial modifications to Eq. (3.6) were studied in the hope of achieving an approximate description of SMA behavior for cyclic loading conditions. First, Eqs. (3.5) and (3.6) were reexpressed as

$$\frac{\dot{\beta}}{E} = \alpha \; [\dot{\varepsilon} - \frac{\dot{\sigma}}{E}]$$

Assuming that the initial conditions on σ, β, and ε are all zero, integration yields

$$\frac{\beta}{E} = \alpha[\varepsilon - \frac{\sigma}{E}] = \alpha\varepsilon^{in} \tag{3.7}$$

It is readily seen from this expression that the backstress is a linear function of the inelastic strain ε^{in}.

By modifying Eq. (3.7) it is possible to describe the various aspects of the shape memory material behavior. A modified form of Eq. (3.7) which will allow such a description is arrived at by adding another term to the inelastic strain in Eq. (3.7)

$$\frac{\beta}{E} = \alpha[\varepsilon^{in} + f_T|\varepsilon|^c erf(a\varepsilon)\{u(-\dot{\varepsilon}\varepsilon)\}] \tag{3.8}$$

where f_T, a and c are material constants. The constant f_T is included to allow for the patterns of hysteretic behavior which are observed in SMA's over varying temperatures. Note that the last term in Eq. (3.8) also contains

the unit step function having the argument $-\dot{\epsilon}\epsilon$, i.e. $\{u(-\dot{\epsilon}\epsilon)\}$. Thus the unit step function will activate the added term only during unloading processes. As such, the ascending branches of the hysteresis loop will be unaffected by the added term. However, when on a descending branch (unloading portion of the stress-strain curve) the added term will contribute to the backstress and will allow for SMA stress-strain descriptions. Examples of such descriptions will be made in Section 5.3 of this report. The motivation for selecting this particular form of the backstress arises from the requirement of zero residual strain which is necessary when describing superelastic material behavior. Thus a backstress function is needed which, when used with Eq. (3.5), will force the σ-ϵ curve to pass through the origin upon unloading for superelastic behavior (refer again to Figure 1-1b). The computational results presented in Section 5.3 will show that when the constants of the function $f_T |\epsilon|^C \text{erf } (a\epsilon)$ are properly selected, the numerical solutions of Eqs. (3.5) and (3.8) will give σ-ϵ behavior characteristic of the superelastic material. Thus, a one dimensional model which will approximately reproduce SMA behavior is given by Eqs. (3.5) and (3.8). These equations are now rewritten for clarity

$$\dot{\epsilon} = \frac{\dot{\sigma}}{E} = |\dot{\epsilon}| \; \left(\frac{\sigma-\beta}{Y}\right)^n \tag{3.9}$$

$$\beta = E\alpha[\epsilon^{in} + f_T|\epsilon|^C \text{erf}(a\epsilon)\{u(-\dot{\epsilon}\epsilon)\}] \tag{3.10}$$

The numerical computations which demonstrate the cyclic behavior of the models of plastic hysteretic behavior and SMA hysteretic behavior, as given by Eqs. (3.5) and (3.6) and Eqs. (3.9) and (3.10) respectively, will be presented in Section 5 of this report. However, before proceeding to such

computations, these two models will be extended to three dimensions so as to allow for multiaxial formulations.

SECTION 4

EXTENSION OF 1D HYSTERETIC MODELS TO 3D

4.1 Introduction

When considering seismically induced horizontal ground motion in one dimension, a variety of important structural response quantities can be calculated by utilizing simple building models where the superstructure is of the shear type. Examples of such studies which include base isolation are given in [7] and [16]. In these studies the energy absorbing device located at the structural base is typically modeled using the one dimensional hysteretic equations of Wen [6] or Ozdemir [13]. If one wishes to account for multidimensional effects in base isolation devices, a three dimensional, representation of the hysteretic behavior is then needed. To allow for such possibilities, an extension of Ozdemir's model given by Eqs. (3.5) and (3.6) will be made to a three dimensional tensor representation. The same extension will be made for the proposed hysteretic model of SMA behavior.

4.2 Extension of Ozdemir's Model to 3D

To begin, Eqs. (3.5) and (3.6) are rewritten so that the restriction on the overstress power n is removed, i.e. n will no longer be restricted to odd integer values. This is done following a standard convention [17] and Eqs. (3.5) and (3.6) become

$$\dot{\varepsilon}_{11} = \frac{\dot{\sigma}_{11}}{E} + \left|\dot{\varepsilon}_{11}\right| \left|\frac{\sigma_{11} - \beta_{11}}{Y}\right|^{n-1} \left(\frac{\sigma_{11} - \beta_{11}}{Y}\right) \tag{4.1}$$

$$\dot{\beta}_{11} = E\alpha \left|\dot{\varepsilon}_{11}\right| \left|\frac{\sigma_{11} - \beta_{11}}{Y}\right|^{n-1} \left(\frac{\sigma_{11} - \beta_{11}}{Y}\right) \tag{4.2}$$

where the subscripts 11 represent uniaxial behavior in the x direction of a Cartesian coordinate system. The only restriction now remaining on n is that it have values such that $n \geq 1$.

In Shames and Cozzarelli [18] a procedure for extending one dimensional rate laws to a three dimensional tensor expression is presented for the case of steady creep. The extension of Eqs. (4.1) and (4.2) to three dimensions will follow this procedure. Considering Eq. (4.1), the first term on the right hand side is the elastic part of the strain rate and the second term is the nonlinear inelastic part of the strain rate. In the subsequent development the inelastic component of the strain will be taken as incompressible. This is a standard assumption which arises from the commonly held belief that both creep and plastic behavior result from the movement of dislocations in the microstructure and no volume change is associated with this effect. In the extension of Eq. (4.1) the elastic component of the one dimensional strain proceeds to the three dimensional form of elasticity theory, i.e.

$$\varepsilon_{ij}^{el} = \frac{1+\nu}{E}\sigma_{ij} - \frac{\nu}{E}\sigma_{kk}\delta_{ij} \qquad (4.3)$$

where ε_{ij}^{el} is the elastic component of the total strain tensor, σ_{ij} is the stress tensor, E is Young's modulus, ν is the elastic Poisson ratio, and δ_{ij} is the Kronecker delta.

The inelastic component of the one dimensional expression for the strain rate is now rewritten for clarity

$$\dot{\varepsilon}_{11}^{in} = |\dot{\varepsilon}_{11}| \left|\frac{\sigma_{11} - \beta_{11}}{Y}\right|^{n-1} (\frac{\sigma_{11} - \beta_{11}}{Y}) \qquad (4.4)$$

Extending this quantity to three dimensions now requires a number of steps. In the process, Eq. (4.4) is first rewritten in terms of deviator quantities that pertain to the uniaxial test. Also, it will be assumed for a moment that

the total strain rate appearing in this inelastic term is incompressible. This assumption is made so that it will be possible to extend the quantity $|\dot{\varepsilon}_{11}|$ to three dimensions without considering variable Poisson effects. When considering compressible materials, the value of the Poisson ratio becomes variable once inelastic deformation takes place and it is then unclear how an extension to 3D should proceed. Once the extension process is completed the assumption will be removed and the result will be taken to be approximate for cases which include compressibility effects.

When considering the uniaxial test, Eq. (4.4) may be rewritten as

$$\dot{\varepsilon}_{11}^{in} = \left| \frac{3}{2} \dot{e}_{11} \right| \left| \frac{\frac{3}{2}(s_{11} - b_{11})}{Y} \right|^{n-1} \left(\frac{s_{11} - b_{11}}{Y} \right)$$

where s_{11} is the uniaxial component of the stress deviator tensor, b_{11} is the uniaxial component of the backstress deviator tensor, and $\dot{e}_{11}$ is the uniaxial component of the total strain rate deviator tensor. Following the procedure for extending uniaxial constitutive relations to three dimensions given in [18], quantities that are operated on by the absolute value are extended to three dimensions by generalization to the positive square root of an associated invariant quantity. As such the following extensions are made

$$\frac{3}{2}\dot{e}_{11} \longrightarrow (3K_2)^{1/2} \qquad K_2 = \frac{1}{2} \dot{e}_{ij} \dot{e}_{ij}$$

$$\left| \frac{\frac{3}{2}(s_{11} - b_{11})}{Y} \right| \longrightarrow (3J_2^o) \qquad J_2^o = \frac{1}{2} \left(\frac{s_{ij} - b_{ij}}{Y} \right) \left(\frac{s_{ij} - b_{ij}}{Y} \right)$$

where K_2 is the second invariant of the strain rate deviator tensor

4-3

$(\dot{e}_{ij} = \dot{\varepsilon}_{ij} - \frac{1}{3} \dot{\varepsilon}_{kk} \delta_{ij})$ and J_2^0 is the second invariant of the dimensionless overstress deviator tensor. The overstress deviator tensor is now formally defined as $s_{ij} - b_{ij}$ where s_{ij} is the stress deviator tensor $(s_{ij} = \sigma_{ij} - \frac{1}{3} \sigma_{kk} \delta_{ij})$ and b_{ij} is the backstress deviator tensor $(b_{ij} = \beta_{ij} - \frac{1}{3} \beta_{kk} s_{ij})$. The remaining extensions of the overstress and the inelastic strain rate will complete the steps of the process

$$\varepsilon_{11}^{in} \quad \dashrightarrow \quad \varepsilon_{ij}^{in}$$

$$s_{11} \quad \dashrightarrow \quad s_{ij}$$

$$b_{11} \quad \dashrightarrow \quad b_{ij}$$

Thus the extended form of Eq. (4.4) is

$$\dot{\varepsilon}_{ij}^{in} = (3K_2)^{1/2} (3J_2^0)^{\frac{n-1}{2}} \left(\frac{s_{ij} - b_{ij}}{Y}\right) \tag{4.5}$$

Now, the previously imposed restriction that the total strain be incompressible will be removed and Eq. (4.5) will be taken to give the approximate inelastic strain rate for conditions of general strain fields and strain rates of compressible materials. Note, however, that this does not imply that the inelastic strain resulting from Eq. (4.5) is also not incompressible. It can be readily be seen from the trace of Eq. (4.5) that no volume rate dilation is possible for the inelastic component of the strain and thus there is no volume change associated with the inelastic component of strain. Now, the constitutive relation for the total strain rate tensor composed of linear elastic and nonlinear inelastic parts is as follows:

$$\dot{\varepsilon}_{ij} = \frac{1+\nu}{E} \dot{\sigma}_{ij} - \frac{\nu}{E} \dot{\sigma}_{kk}\delta_{ij} + (3K_2)^{1/2} (3J_2^o)^{\frac{n-1}{2}} (\frac{s_{ij} - b_{ij}}{Y}) \qquad (4.6)$$

Next, the expression that defines the evolution of the backstress (Eq. (4.2)) also needs to be extended to three dimensions. Eq. (3.10) is first recast into an equivalent expression which is deduced by considering Eqs. (3.9) and (3.10) together. The specific form of the recast equation is

$$\dot{\beta}_{11} = E\alpha \ (\dot{\varepsilon}_{11} - \frac{\dot{\sigma}_{11}}{E})$$

It is then immediately evident that

$$\dot{\beta}_{11} = E\alpha \ \dot{\varepsilon}_{11}^{in}$$

which, when re-expressed in terms of the deviator expressions of the uniaxial test, becomes

$$\dot{b}_{11} = \frac{2}{3} \ E\alpha\dot{\varepsilon}_{11}^{in}$$

In the extension to three dimensions

$$\dot{b}_{11} \ \longrightarrow \ \dot{b}_{ij}$$

$$\dot{\varepsilon}^{in} \ \longrightarrow \ \dot{\varepsilon}_{ij}^{in}$$

Therefore

$$\dot{b}_{ij} = \frac{2}{3} \ E\alpha\dot{\varepsilon}_{ij}^{in}$$

or

$$\dot{b}_{ij} = \frac{2}{3} E\alpha \ (3K_2)^{1/2} \ (3J_2)^{\frac{n-1}{2}} \ (\frac{s_{ij} - b_{ij}}{Y}) \qquad (4.7)$$

Therefore, the fully extended formulation expressed in terms of the strain rate tensor is given by Eqs. (4.6) and (4.7). This formulation is now rewritten for clarity

$$\dot{\varepsilon}_{ij} = \frac{1+\nu}{E} \dot{\sigma}_{ij} - \frac{\nu}{E} \dot{\sigma}_{kk} \delta_{ij} + (3K_2)^{1/2} \ (3J_2^o)^{\frac{n-1}{2}} \ (\frac{s_{ij} - b_{ij}}{Y}) \qquad (4.8a)$$

$$\dot{b}_{ij} = \frac{2}{3} E\alpha \ (3K_2)^{1/2} \ (3J_2^o)^{\frac{n-1}{2}} \ (\frac{s_{ij} - b_{ij}}{Y}) \qquad (4.8b)$$

where

$$s_{ij} = \sigma_{ij} - \frac{1}{3} \sigma_{kk} \ \delta_{ij}$$

$$b_{ij} = \beta_{ij} - \frac{1}{3} \beta_{kk} \ \delta_{ij}$$

$$e_{ij} = \varepsilon_{ij} - \frac{1}{3} \varepsilon_{kk} \ \delta_{ij}$$

$$K_2 = \frac{1}{2} \dot{e}_{ij} \dot{e}_{ij}$$

$$J_2^o = \frac{1}{2} \ (\frac{s_{ij} - b_{ij}}{Y}) \ (\frac{s_{ij} - b_{ij}}{Y})$$

Now, let the formulation of Eqs. (4.8) be examined for the special case of uniaxial behavior. In this examination the changes in volume which

result from the Poisson effect will be included. For the case of the uniaxial test the states of stress, backstress, and strain rate as well as the associated deviatoric states are as follows:

$$\sigma_{ij} = \begin{bmatrix} \sigma_{11} & 0 & 0 \\ 0 & 0 & 0 \\ 0 & 0 & 0 \end{bmatrix} \qquad s_{ij} = \begin{bmatrix} \frac{2}{3}\sigma_{11} & 0 & 0 \\ 0 & -\frac{1}{3}\sigma_{11} & 0 \\ 0 & 0 & -\frac{1}{3}\sigma_{11} \end{bmatrix}$$

$$\beta_{ij} = \begin{bmatrix} \beta_{11} & 0 & 0 \\ 0 & 0 & 0 \\ 0 & 0 & 0 \end{bmatrix} \qquad b_{ij} = \begin{bmatrix} \frac{2}{3}\beta_{11} & 0 & 0 \\ 0 & -\frac{1}{3}\beta_{11} & 0 \\ 0 & 0 & -\frac{1}{3}\beta_{11} \end{bmatrix}$$

$$\dot{\varepsilon}_{ij} = \begin{bmatrix} \dot{\varepsilon}_{11} & 0 & 0 \\ 0 & -\gamma\dot{\varepsilon}_{11} & 0 \\ 0 & 0 & -\gamma\dot{\varepsilon}_{11} \end{bmatrix}$$

$$\dot{e}_{ij} = \begin{bmatrix} \frac{2}{3}(1+\gamma)\dot{\varepsilon}_{11} & 0 & 0 \\ 0 & -\frac{1}{3}(1+\gamma)\dot{\varepsilon}_{11} & 0 \\ 0 & 0 & -\frac{1}{3}(1+\gamma)\dot{\varepsilon}_{11} \end{bmatrix}$$

where σ_{11} is the uniaxial stress, β_{11} is the uniaxial backstress, $\dot{\varepsilon}_{11}$ is the uniaxial strain rate, and γ is the variable Poisson effect associated with the lateral deformation rate.

It can be shown that γ is as follows for this uniaxial case

$$\gamma = \frac{1}{2} - \frac{1}{E}\left(\frac{1}{2} - \nu\right)\frac{d\sigma_{11}}{d\varepsilon_{11}} \tag{4.9}$$

By carrying out the necessary mathematical manipulations and simplifications

$$(3K_2)^{1/2} = (1+\gamma) \, |\dot{\varepsilon}_{11}|$$

$$(3J_2^o)^{\frac{n-1}{2}} = \left|\frac{\sigma_{11} - \beta_{11}}{Y}\right|^{n-1}$$

$$\gamma = \frac{\nu+1}{1 - \frac{2}{3}(\frac{1}{2}-\nu)\left[\text{sgn}(\dot{\varepsilon}_{11}) \, \left|\frac{\sigma_{11} - \beta_{11}}{Y}\right|^{n-1}(\frac{\sigma_{11} - \beta_{11}}{Y})\right]} - 1$$

Thus the uniaxial components of Eqs. (4.8) are as follows:

$$\dot{\varepsilon}_{11} = \frac{\dot{\sigma}_{11}}{E} + \frac{2}{3} \, (1+\gamma) \, \left|\dot{\varepsilon}_{11}\right| \, \left|\frac{\sigma_{11} - \beta_{11}}{Y}\right|^{n-1} (\frac{\sigma_{11} - \beta_{11}}{Y}) \qquad (4.10)$$

$$\dot{\beta}_{11} = \frac{2}{3} \, E\alpha(1+\gamma) \, \left|\dot{\varepsilon}_{11}\right| \, \left|\frac{\sigma_{11} - \beta_{11}}{Y}\right|^{n-1} (\frac{\sigma_{11} - \beta_{11}}{Y}) \qquad (4.11)$$

If an incompressible material is considered, i.e. a material having $\nu = 1/2$, the variable Poisson ratio for the strain rate will become constant according to Eq. (4.9), i.e. $\gamma = 1/2$. Therefore for the special case of an incompressible material Eqs. (4.10) and (4.11) become

$$\dot{\varepsilon}_{11} = \frac{\dot{\sigma}_{11}}{E} + \left|\dot{\varepsilon}_{11}\right| \, \left|\frac{\sigma_{11} - \beta_{11}}{Y}\right|^{n-1} (\frac{\sigma_{11} - \beta_{11}}{Y}) \qquad (4.12)$$

$$\dot{\beta}_{11} = E\alpha \, \left|\dot{\varepsilon}_{11}\right| \, \left|\frac{\sigma_{11} - \beta_{11}}{Y}\right|^{n-1} (\frac{\sigma_{11} - \beta_{11}}{Y}) \qquad (4.13)$$

Comparison of Eqs. (4.12) and (4.13) with Eqs. (4.1) and (4.2) reveal that Ozdemir's model results from the tensor formulation of Eqs. (4.8) for the special case of a uniaxial test applied to an incompressible material. In Section 5, results of numerical calculations will be used to show the behavior of this model.

4.3 Extension of Proposed Model of SMA Behavior to 3D

Next the proposed model of SMA behavior, Eqs. (3.9) and (3.10), will be extended to three dimensions. The proposed equations as given by Eqs. (3.9) and (3.10) are now rewritten

$$\dot{\varepsilon}_{11} = \frac{\dot{\sigma}_{11}}{E} + \left|\dot{\varepsilon}_{11}\right| \left|\frac{\sigma_{11} - \beta_{11}}{Y}\right|^{n-1} (\frac{\sigma_{11} - \beta_{11}}{Y}) \tag{4.14}$$

$$\frac{\beta_{11}}{E} = \alpha[\varepsilon_{11}^{in} + f_T|\varepsilon_{11}|^C erf(a\varepsilon_{11})\{u(-\varepsilon_{11}\dot{\varepsilon}_{11})\}] \tag{4.15}$$

Again, removing the restriction on the overstress power n, and extending Eq. (4.14) to three dimensions as before yields Eq. (4.8a), i.e.

$$\dot{\varepsilon}_{ij} = \frac{1+\nu}{E}\dot{\sigma}_{ij} - \frac{\nu}{E}\dot{\sigma}_{kk}\delta_{ij} + (3K_2)^{1/2} (3J_2^o)^{\frac{n-1}{2}} (\frac{s_{ij} - b_{ij}}{Y})$$

The extension of Eq. (4.15) will be made assuming a uniform temperature throughout the material. As was done in the previous extension, Eq. (4.15) is first recast in terms of the uniaxial components of deviator tensors again with the momentary assumption of incompressible material behavior. Thus Eq. (4.15) becomes

$$b_{11} = \frac{2}{3} E\alpha [\varepsilon_{11}^{in} + f_T |e_{11}|^C erf (ae_{11})\{u(-\varepsilon_{11}\dot{\varepsilon}_{11})\}] \tag{4.16}$$

To facilitate the extension, the error function in Eq. (4.16) is replaced by its series expansion [19]

$$erf(x) = \frac{2}{\sqrt{\pi}} \sum_{k=0}^{\infty} \frac{(-1)^k}{k!(2k+1)} x^{2k+1}$$

Therefore the function erf (ae_{11}) can be re-expressed as

$$erf(ae_{11}) = \frac{2a}{\sqrt{\pi}} e_{11} \sum_{k=0}^{\infty} \frac{(-1)^k a^{2k}}{k!(2k+1)} \left| e_{11} \right|^{2k}$$

Now Eq. (4.16) can be rewritten as

$$b_{11} = [\varepsilon_{11}^{in} + g_T\{u(-\dot{\varepsilon}_{11}\dot{\varepsilon}_{11})\} \left| \frac{3}{2}e_{11} \right|^c e_{11} \sum_{k=0}^{\infty} \frac{(-1)^k (2a/3)^{2k}}{k!(2k+1)} \left| \frac{3}{2}e_{11} \right|^{2k}] \qquad (4.17)$$

where

$$g_T = \left(\frac{2}{3}\right)^c \left(\frac{2a}{\sqrt{\pi}}\right) f_T$$

The same extension methodology can now be used for Eq. (4.17), i.e.

$$b_{11} \dashrightarrow b_{ij}$$

$$s_{11} \dashrightarrow s_{ij}$$

$$\frac{3}{2} e_{11} \dashrightarrow (3I_2)^{1/2} \qquad\qquad I_2 = \frac{1}{2} e_{ij}e_{ij}$$

$$\{u(-\dot{\varepsilon}_{11}\dot{\varepsilon}_{11})\} \dashrightarrow \{u(-\dot{I}_2)\}$$

where the quantity I_2 is the second invariant of the strain deviator tensor and $\dot{I}_2 = dI_2/dt$. Again the restriction that the material be incompressible is now removed and the formulation for the SMA behavior in a three dimensional rate expression with internal variable of backstress is as follows:

$$\dot{\varepsilon}_{ij} = \frac{1+\nu}{E} \dot{\sigma}_{ij} - \frac{\nu}{E} \dot{\sigma}_{kk}\delta_{ij} + (3K_2)^{1/2} (3J_2^o)^{\frac{n-1}{2}} (\frac{s_{ij} - b_{ij}}{Y}) \qquad (4.18)$$

$$b_{ij} = Ex \; [\varepsilon_{ij}^{in} + g_T e_{ij}\{u(-\dot{I}_2)\} \; (3I_2)^{c/2} \sum_{k=0}^{\infty} \frac{(-1)^k (2a/3)^{2k}}{k!(2k+1)} (3I_2)^k] \qquad (4.19)$$

To examine the formulation given by Eqs. (4.18) and (4.19) let the special case of the uniaxial test now be considered. For this case

$$s_{ij} = \begin{bmatrix} \frac{2}{3}\sigma_{11} & 0 & 0 \\ 0 & -\frac{1}{3}\sigma_{11} & 0 \\ 0 & 0 & -\frac{1}{3}\sigma_{11} \end{bmatrix} \qquad b_{ij} = \begin{bmatrix} \frac{2}{3}\beta_{11} & 0 & 0 \\ 0 & -\frac{1}{3}\beta_{11} & 0 \\ 0 & 0 & -\frac{1}{3}\beta_{11} \end{bmatrix}$$

$$\varepsilon_{ij} = \begin{bmatrix} \varepsilon_{11} & 0 & 0 \\ 0 & -\delta\varepsilon_{11} & 0 \\ 0 & 0 & -\delta\varepsilon_{11} \end{bmatrix}$$

$$e_{ij} = \begin{bmatrix} \frac{2}{3}(1+\delta)\varepsilon_{11} & 0 & 0 \\ 0 & -\frac{1}{3}(1+\delta)\varepsilon_{11} & 0 \\ 0 & 0 & -\frac{1}{3}(1+\delta)\varepsilon_{11} \end{bmatrix}$$

where δ is the variable Poisson ratio associated with lateral deformation. It can be shown that δ is as follows:

$$\delta = \frac{1}{2} - \frac{1}{E} \left(\frac{1}{2} - \nu\right) \frac{\sigma_{11}}{\varepsilon_{11}}$$

for this special case of the uniaxial test.

Carrying out the computations for the invariant I_2 it is found that

$$I_2 = \frac{1}{3} (1+\delta)^2 \varepsilon_{11}^2$$

$$\dot{I}_2 = \frac{1}{3} (1+\delta)(1+\gamma)\varepsilon_{11}\dot{\varepsilon}_{11}$$

Therefore

$$(3I_2)^{C/2} = [(1+\delta)|\varepsilon_{11}|]^C$$

$$\{u(-\dot{I}_2)\} = \{u(-\frac{1}{3}(1+\delta)(1+\gamma)\varepsilon_{11}\dot{\varepsilon}_{11})\} = \{u(-\varepsilon_{11}\dot{\varepsilon}_{11})\}$$

Also, the series expansion in Eq. (4.19) reduces to

$$\sum_{k=0}^{\infty} \frac{(-1)^k \left(\frac{2}{3}a\right)^{2k}}{k! \ (2k+1)} (3I_2)^k = \frac{\frac{\sqrt{\pi}}{2}}{\frac{2}{3}a(1+\delta)\varepsilon_{11}} \ \text{erf} \ \left(\frac{2}{3} a (1+\delta)\varepsilon_{11}\right)$$

After simplification Eq. (4.19) reduces to the following for the uniaxial test

$$\beta_{11} = E\alpha \ [\varepsilon_{11}^{in} + \frac{3}{2} \frac{\sqrt{\pi}}{2a} g_T \ [(1+\delta)|\varepsilon_{11}|]^C \ \text{erf}(\frac{2}{3}a(1+\delta)\varepsilon_{11})\{u(-\varepsilon_{11}\dot{\varepsilon}_{11})\}]$$

Now, upon considering the case of an incompressible material, i.e. a material having $\nu = 1/2$, it is evident that $\delta = 1/2$. Upon using the

definition of g(T) given following Eq. (4.17) and simplifying, the expression for β becomes

$$\beta_{11} = E\alpha \ [\varepsilon_{11}^{in} + f_T \ |\varepsilon_{11}|^C \ erf(a\varepsilon_{11})\{u(-\varepsilon_{11}\dot{\varepsilon}_{11})\}]$$

When considering the result of Eq. (4.18) for this special case, it has been shown previously that Eq. (4.12) will result. Therefore Eqs. (4.18) and (4.19) have reduced to the following for the special case of the uniaxial test applied to an incompressible material:

$$\dot{\varepsilon}_{11} = \frac{\dot{\sigma}_{11}}{E} + \left|\dot{\varepsilon}_{11}\right| \ \left|\frac{\sigma_{11} - \beta_{11}}{Y}\right|^{n-1} \ (\frac{\sigma_{11} - \beta_{11}}{Y}) \tag{4.20}$$

$$\beta_{11} = E\alpha \ [\varepsilon_{11}^{in} + f_T \ |\varepsilon_{11}|^C \ erf(a\varepsilon_{11})\{u(-\varepsilon_{11}\dot{\varepsilon}_{11})\}] \tag{4.21}$$

Thus it is seen that the original expressions used to make the extension to three dimensions are the result of the special case of Eqs. (4.18) and (4.19) for an incompressible material in the uniaxial test.

In the next section the results of numerical computations will be used to show how the model of SMA behavior in one dimension, Eqs. (4.20) and (4.21), exhibits the various aspects of that particular material behavior.

COMPUTATIONAL RESULTS

5.1 Introduction

In this section some results of numerical computations will be presented for the models of hysteretic behavior which are presently under consideration. In the cases presented here, one dimensional uniaxial cyclic loading under strain control will be considered. Both Ozdemir's model of hysteretic material behavior and the proposed model of SMA hysteretic material behavior will be used in the presentation of numerical results.

5.2 Results for Ozdemir's Model

First, Ozdemir's model of one dimensional hysteretic stress-strain material behavior is considered. This model is given by Eqs. (4.12) and (4.13). The equations are rearranged and the subscripts are dropped, to give the stress-rate as follows:

$$\dot{\sigma} = E \left[\dot{\varepsilon} - |\dot{\varepsilon}| \left| \frac{\sigma - \beta}{Y} \right|^{n-1} (\frac{\sigma - \beta}{Y}) \right] \tag{5.1}$$

$$\dot{\beta} = E \, \alpha \, |\dot{\varepsilon}| \left| \frac{\sigma - \beta}{Y} \right|^{n-1} (\frac{\sigma - \beta}{Y}) \tag{5.2}$$

Given a set of material data (E,Y,α,n) as input, a FORTRAN algorithm is used to solve the above equations numerically with fourth order Runge-Kutta integration. The initial conditions are taken to be zero at the onset of calculations.

Material data for A-36 structural steel, was taken from [20] for Young's modulus, axial initial Yield strength, and the plastic modulus, i.e. E, Y, and Ey respectively. The material data is given below

Material Data for A-36

Material Property	Symbol	Value
Young's modulus	E	28500 ksi
Axial initial Yield stress	Y	30 ksi
Plastic modulus	E_y	550 ksi

Using the definition of α given following Eq. (4.4) it is found that

$$\alpha = .0197$$

for A-36 steel.

Using this data, Eqs. (5.1) and (5.2) were integrated numerically and the results for the stress-strain material behavior were plotted graphically using the computer. A series of plots shown in Figures 5-1 to 5-4 show the effect of the overstress power n on the shape of the hysteresis loop. For n=1 the loop is well rounded as seen in Figure 5-1. As n increases in value, the transition from elastic to plastic behavior becomes much more pronounced as shown in Figures 5-2, 5-3 and 5-4 for n = 5, 9 and 15 respectively. In fact Figure 5-4 nearly replicates elastic-plastic material behavior with linear work hardening (also called bilinear behavior).

Since the transition from elastic to plastic material behavior is sharpest in Figure 5-4, it is possible to check the initial yield point as given by the model. By examination of Figure 5-4, the yield point can be seen to be in the vicinity of the actual material yield for A-36 steel, i.e. Y = 30 ksi. Thus the actual material yield point is well represented by the model. Also, it can be seen from any of the Figures 5-1 to 5-4 that the Bauschinger effect is manifested with the model. Thus, two important features of physical

$$\varepsilon = A \sin \omega t$$

$$Y = 30 \text{ ksi} \quad \nu = 0.5$$

$$E = 28500 \text{ ksi}$$

$$\alpha = 0.0197 \quad n = 1$$

$$\omega = 1 \quad A = .016$$

Ozdemir's Hysteretic Model
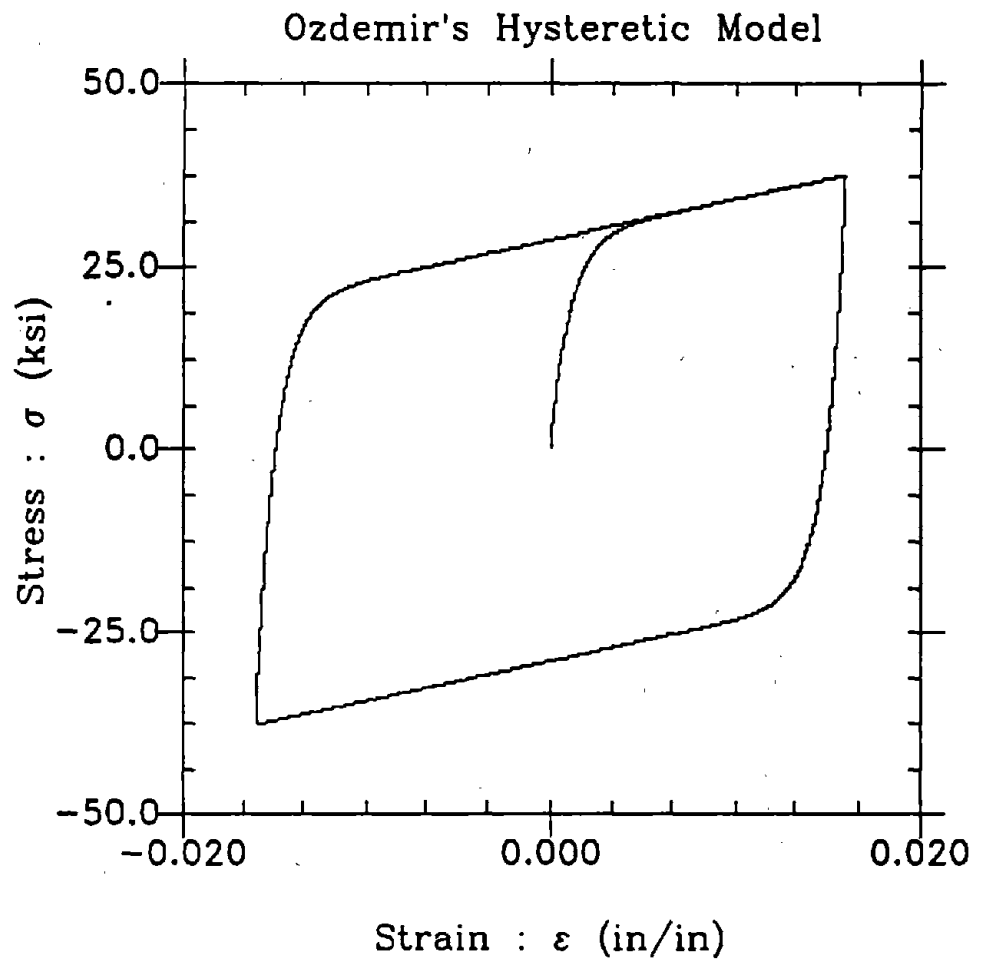
FIGURE 5-1   Smooth Transition from Elastic to Plastic Regime Using Ozdemir's

Model with n = 1

$$\varepsilon \;=\; A \; \sin \; \omega t$$

$$Y \;=\; 30 \; \text{ksi} \quad \nu \;=\; 0.5$$

$$E \;=\; 28500 \; \text{ksi}$$

$$\alpha \;=\; 0.0197 \quad n \;=\; 5$$

$$\omega \;=1 \quad A \;=\; .016$$
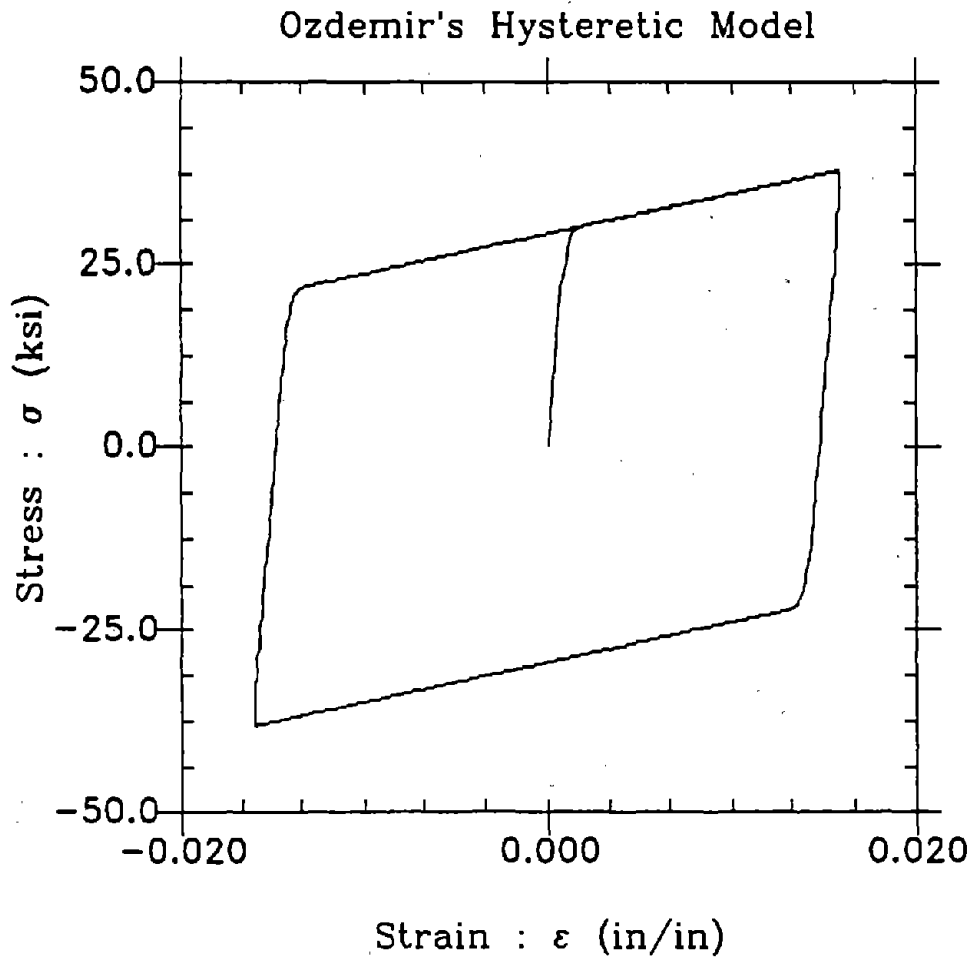
FIGURE 5-2   Ozdemir's Model with n = 5

$$\varepsilon \; = \; A \; \sin \; \omega t$$

$$Y \; = \; 30 \; ksi \quad \nu \; = \; 0.5$$

$$E \; = \; 28500 \; ksi$$

$$\alpha \; = \; 0.0197 \quad n \; = \; 9$$

$$\omega \; = 1 \quad A \; = \; .016$$

Ozdemir's Hysteretic Model
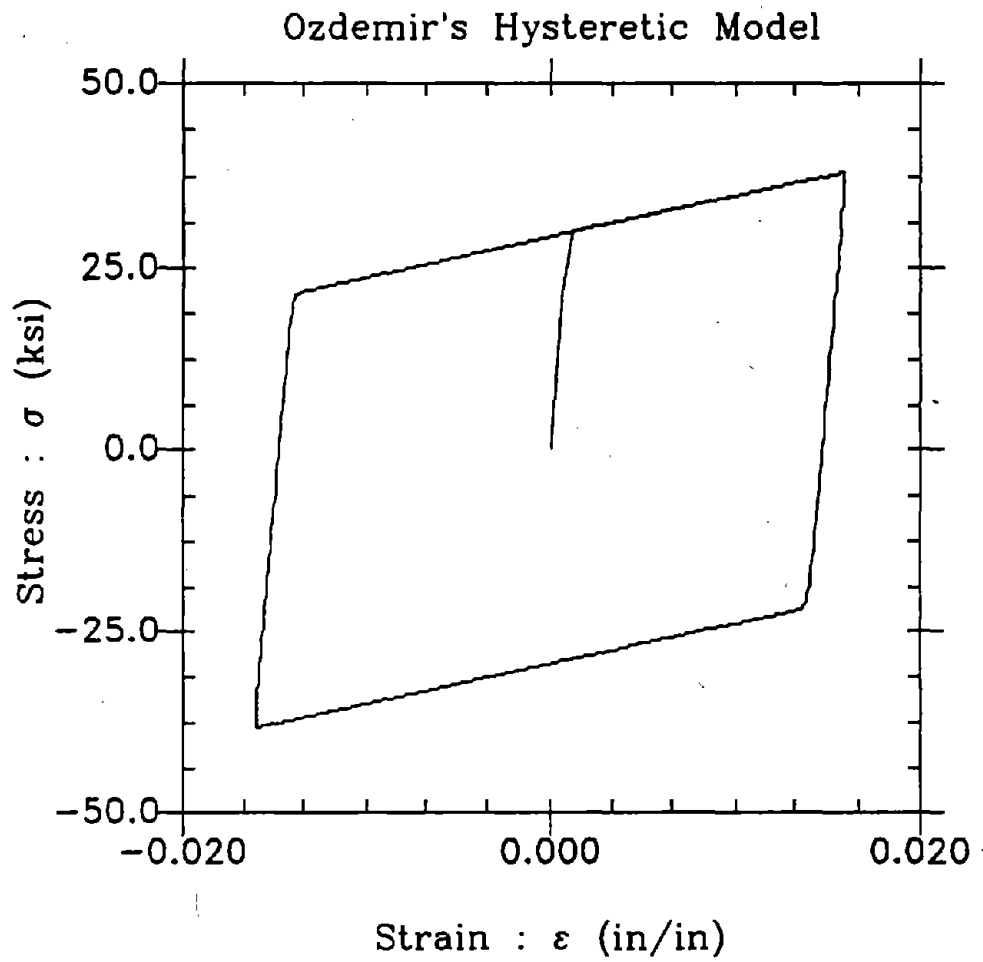
FIGURE 5-3 Ozdemir's Model with n = 9

$$\varepsilon = A \sin \omega t$$

$$Y = 30 \text{ ksi} \quad \nu = 0.5$$

$$E = 28500 \text{ ksi}$$

$$\alpha = 0.0197 \quad n = 15$$

$$\omega = 1 \quad A = .016$$

Ozdemir's Hysteretic Model
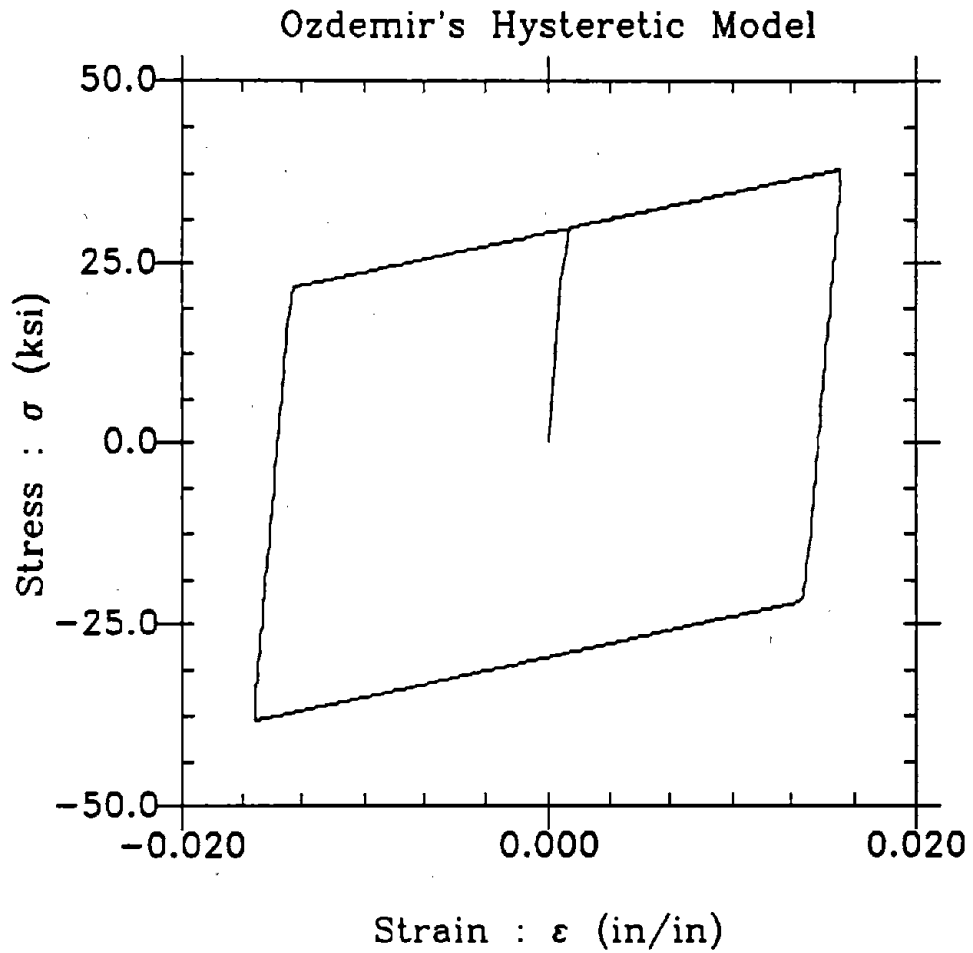
FIGURE 5-4 Ozdemir's Model with n = 15, Bilinear Behavior

material behavior are reproduced by the model (Eqs. (5.1) and (5.2)), namely the material yield point and the Bauschinger effect.

The model is also able to properly reproduce the slope of both the elastic and plastic portions of the stress strain curves, i.e. E and E_y. This is show in Figure 5-5 for n = 15. In this figure the slope of the hysteresic stress-strain curve of Figure 5-4 is plotted. The elastic slope E is correctly reproduced by the model, i.e. E = 28500 ksi. The value of the plastic slope, E_y, cannot be easily read off the plot. However, a check of the data from the numerical calculations gives the plastic slope as 550.6 ksi, a very small departure from the actual material value of E_y = 550 ksi. Thus the values of the elastic and plastic moduli are also reproduced using the hysteretic model. It is therefore possible to characterize one-dimensional hysteretic material behavior easily and accurately using Eqs. (5-1) and (5-2).

5.3 Results for the Proposed Model of SMA Behavior

Next, the model of SMA behavior will be considered. Recall that the proposed equations for SMA one dimensional stress-strain behavior were given by Eqs. (4.20) and (4.21). They are now rewritten here for convenience, and once again the subscripts are dropped.

$$\dot{\sigma} = E \left[\dot{\varepsilon} - |\dot{\varepsilon}| \left| \frac{\sigma-\beta}{Y} \right|^{n-1} \left(\frac{\sigma-\beta}{Y} \right) \right] \tag{5.3}$$

$$\beta = E\alpha \left[\varepsilon^{in} + f_T |\varepsilon|^C \text{erf}(a\varepsilon)\{u(-\dot{\varepsilon}\varepsilon)\} \right] \tag{5.4}$$

The backstress β given by Eq. (5.4) is seen to be the sum of two parts, a term which is linearly dependent on the inelastic strain, and a second term $E\alpha f_T |\varepsilon|^C \text{erf}(a\varepsilon)\{u(-\dot{\varepsilon}\varepsilon)\}$ which is active only during unloading processes. It

$$\varepsilon \;=\; A \;\sin\; \omega t$$

$$Y \;=\; 30 \;\text{ksi} \quad \nu \;=\; 0.5$$

$$E \;=\; 28500 \;\text{ksi}$$

$$\alpha \;=\; 0.0197 \quad n \;=\; 15$$

$$\omega \;=1 \quad A \;=\; .016$$

Slope of Stress–Strain curve for Ozdemir's model
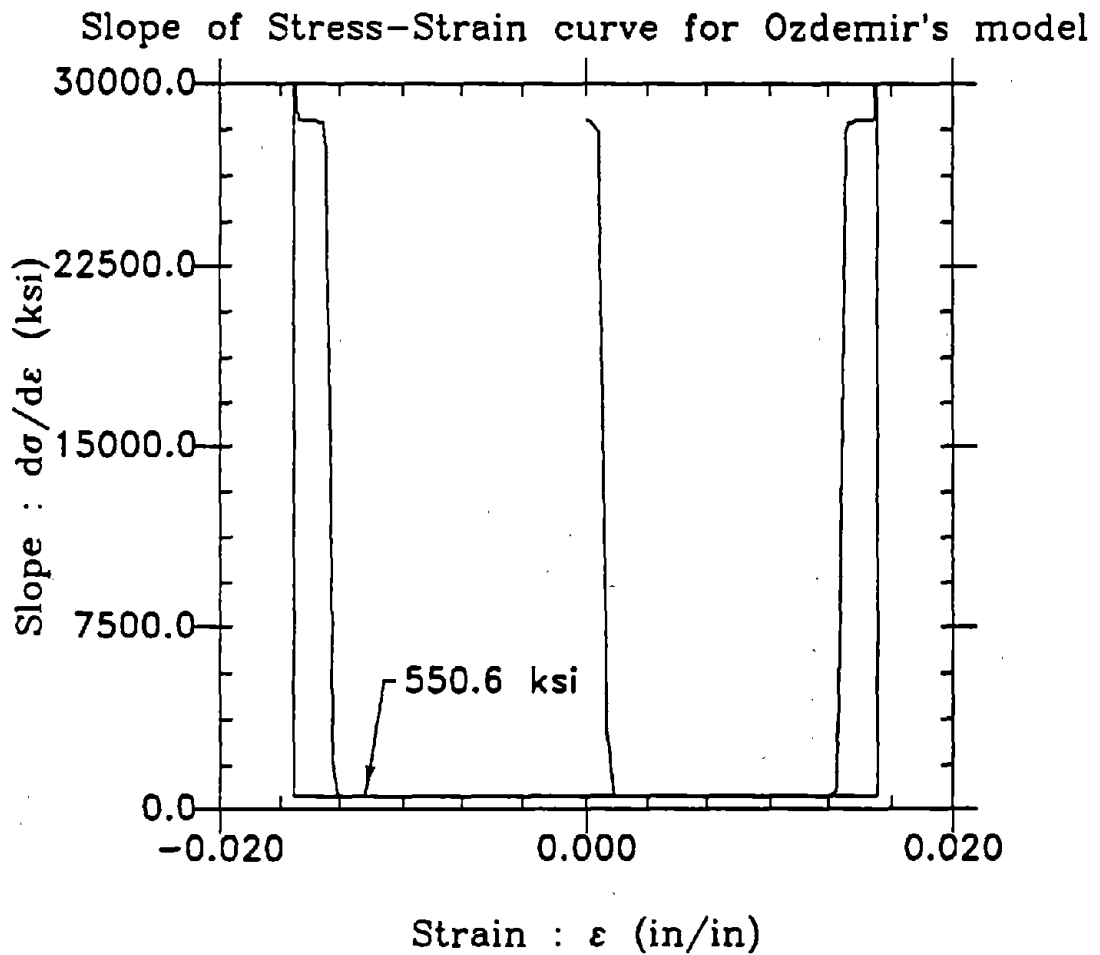
FIGURE 5-5 Slope of Hysteresis Loop with n = 15

is the inclusion of this second term that allows the various patterns of SMA behavior to be reproduced by the model.

Displacement controlled cyclic loading tests of Nickel-Titanium SMA uniaxial specimens are presently being conducted on MTS equipment as part of this research. The forthcoming experimental results will provide a set of data for the hysteretic behavior of these materials. With this data, characterization studies will be made using the model of SMA behavior proposed here. In the present discussion however, the model parameters of Eqs. (5.3) and (5.4) will be selected so as to demonstrate some various types of SMA behavior. Eqs. (5.3) and (5.4) involve the following material constants; E, Y, n, α, f_T, a and c. The constants E and Y represent the elastic modulus and initial axial yield point respectively. The overstress power n controls the sharpness of transition from elastic to inelastic regions of the SMA stress-strain curve. The constant α is used to relate the inelastic modulus to the elastic modulus, and is given by the following equation; $\alpha = E_y/(E-E_y)$ where E_y is the slope of the stress-strain curve following initial axial yielding (i.e. the inelastic modulus of the SMA). Thus the constants E, Y, n, and α are all simple constants and can be determined in a simple one-dimensional testing configuration. With constants f_T, a, and c, the model of Eqs. (5.3) and (5.4) is fully characterized.

Examples of the above model are now presented. For the purposes of model demonstration, the material constants E, Y, and α are selected to be the same as those of A-36 steel, i.e.

$$E = 28500 \text{ ksi}$$

$$Y = 30 \text{ ksi}$$

$$\alpha = 0.0197$$

The overstress power is selected as n = 3, and to begin the discussion the constant f_T is chosen as; $f_T = 0$. This will eliminate the participation of

the term $f_T |\dot\varepsilon|^C \text{erf}(a\varepsilon)\{u(-\dot\varepsilon\varepsilon)\}$ from the backstress. The cyclic loading condition is taken to be a strain controlled test ranging from $\varepsilon = -0.016$ to $\varepsilon = 0.016$. The hysteresis behavior calculated using Eqs. (5.3) and (5.4) for this set of conditions is shown in Figure 5-6. This hysteresis is typical of SMA behavior with $T < M_f$; which can be seen by referring once again to Figure 1-1. Also, note from Figure 1-1 that as the temperature increases the SMA material behavior proceeds to superelastic. A similar procession is also attainable in the proposed model. The conditions previously set forth for Figure 5-6 are also used in Figures 5-7 to 5-10 with the exception that the constant f_T is assigned positive values. Specifically, $f_T = .01, .03, .05,$ and .07 for Figures 5-7 to 5-10 respectively. Now, with $f_T \neq 0$, the shape of the hysteresis pattern changes from that previously given in Figure 5-6. This is due to the changes in backstress β.

Refer to the calculated results shown in Figures 5-7 to 5-10. Note that the hysteresis loop pattern changes in the unloading portions of the loop. When the value of f_T is taken as .07 (Figure 5-10), the hysteresis loop is seen to give a good schematic representation of superelastic SMA behavior wherein martensite forms as the applied stress is increased. Subsequent release of the applied stress causes the martensite to return to its original parent phase with zero residual strain upon unloading.

It is also of interest to examine the proposed SMA model for its capability to properly represent material constants. Specifically, the proposed model should reproduce the initial axial yield, elastic modulus, and inelastic modulus. By examining the plot of hysteresis for large values of n, the yield point can easily be verified. Therefore n = 15 is used in conjunction with E, Y, α, and f_T as used previously in Figure 5-10. That is

$\varepsilon = .016 \sin 1^*t$

$Y = 30 \text{ ksi} \quad \nu = 0.5$

$E = 28500 \text{ ksi}$

$\alpha = 0.0197$

$n = 3$

$a = 2500 \quad c = .001 \quad f_r = 0$

Proposed Hysteretic Model for SMA
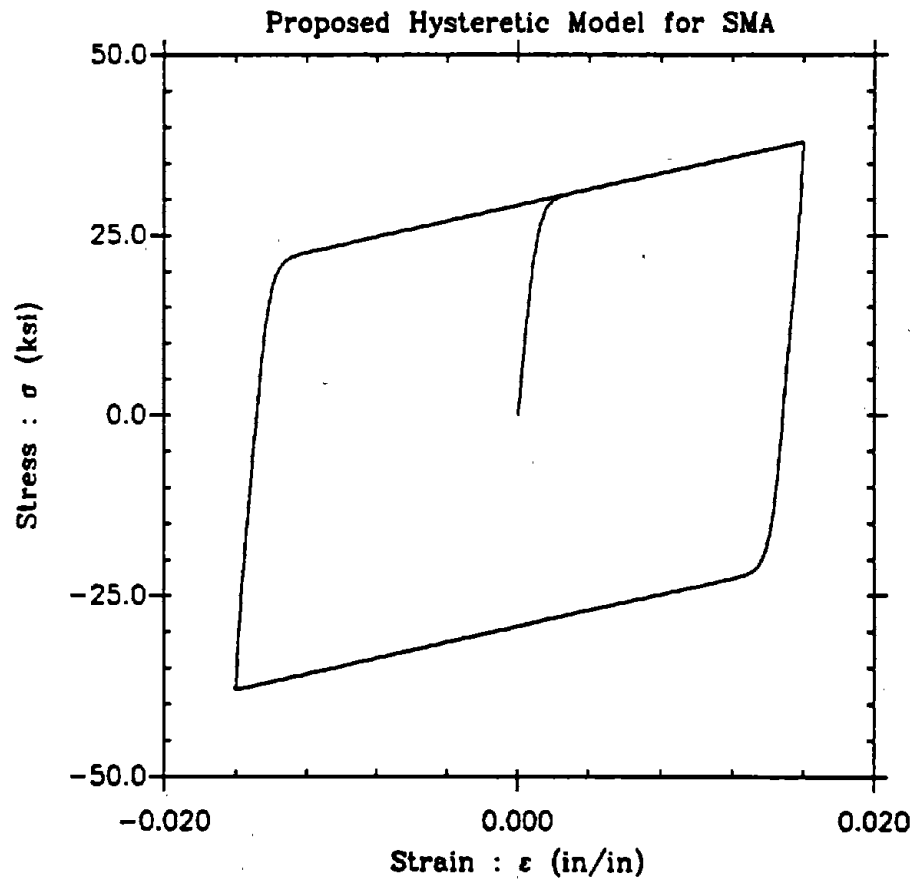
FIGURE 5-6 Cyclic Behavior of SMA Model with $f_T = 0$

$$E = 28000 \text{ ksi}$$

$$Y = 30 \text{ ksi}$$

$$\alpha = 0.0197$$

$$f_T = 0.07$$

The associated behavior predicted by the model under cyclic strain with a = 3500 and c = .0005 is shown in Figure 5-11. Note that the initial axial yield point (which represents the onset of martensite formation) of the material (Y = 30 ksi) is well represented by the model. The slope of the stress-strain curve of Figure 5-11 is plotted in Figure 5-12. Note that the elastic and inelastic slopes of the material (E and E_y) are also well represented by the proposed model. Thus the proposed model of one-dimensional SMA behavior may be a useful analytical tool for the prediction of stress-strain response in fully characterized SMA's.

$\varepsilon = .016 \sin 1^{\bullet}t$

$Y = 30$ ksi $\quad \nu = 0.5$

$E = 28500$ ksi

$\alpha = 0.0197$

$n = 3$

$a = 2500 \quad c = .001 \quad f_{\tau} = .01$

Proposed Hysteretic Model for SMA
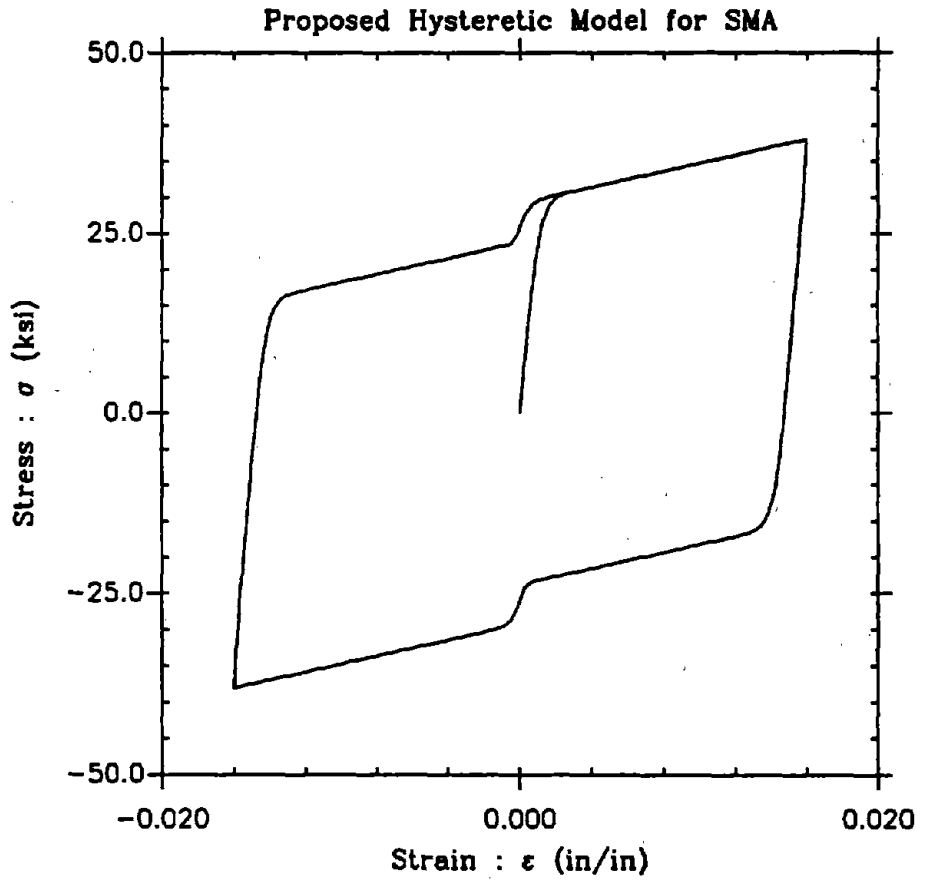
FIGURE 5-7   Cyclic Behavior of SMA Model with $f_T = 0.01$

$\varepsilon = .016 \sin 1^{\circ}t$

$Y = 30 \text{ ksi} \quad \nu = 0.5$

$E = 28500 \text{ ksi}$

$\alpha = 0.0197$

$n = 3$

$a = 2500 \quad c = .001 \quad f_{T} = .03$

Proposed Hysteretic Model for SMA
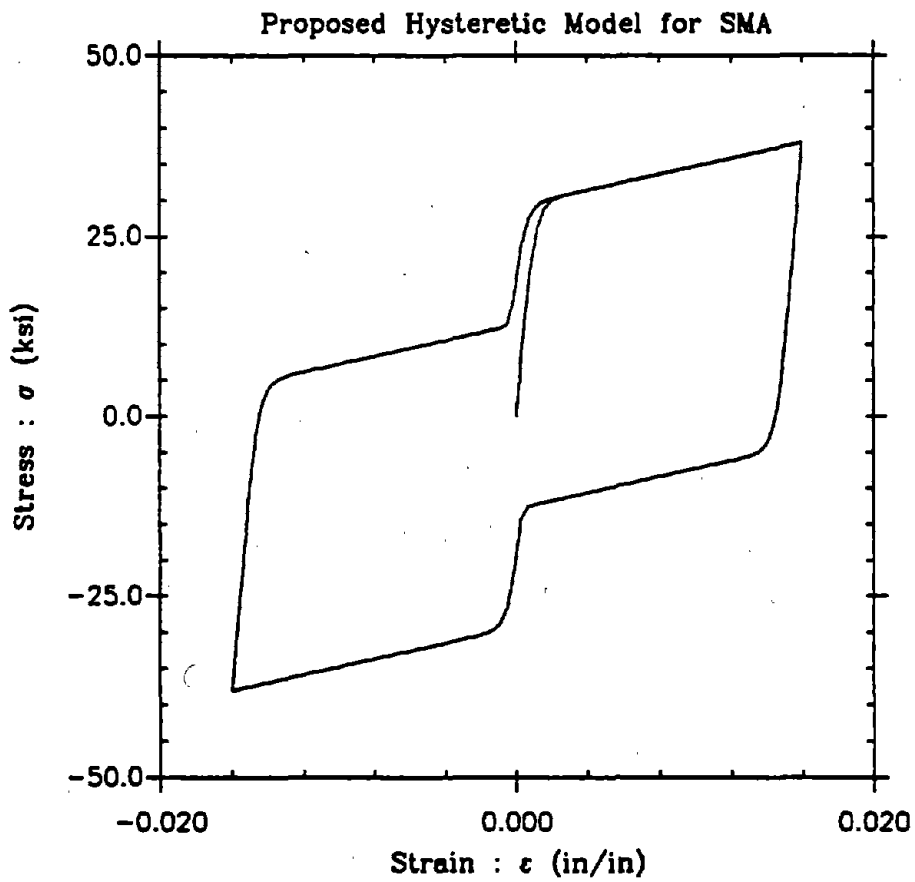
FIGURE 5-8 Cyclic Behavior of SMA Model with $f_{T} = 0.03$

$\varepsilon = .016 \sin 1 \cdot t$

$Y = 30$ ksi $\nu = 0.5$

$E = 28500$ ksi

$\alpha = 0.0197$

$n = 3$

$a = 2500$ $c = .001$ $f_T = .05$

Proposed Hysteretic Model for SMA
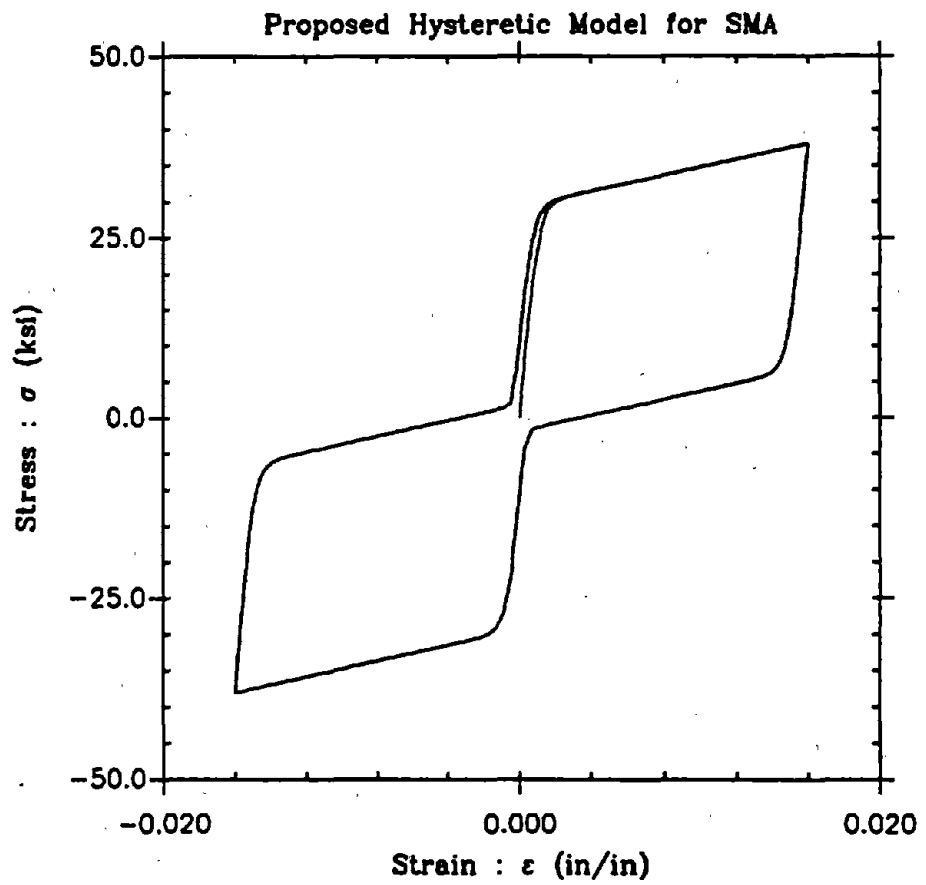
FIGURE 5-9 Cyclic Behavior of SMA Model with $f_T = 0.05$

ε = .016 sin 1*t

Y = 30 ksi ν = 0.5

E = 28500 ksi

α = 0.0197

n = 3

a = 2500   c = .001 f_τ =.07

Proposed Hysteretic Model for SMA
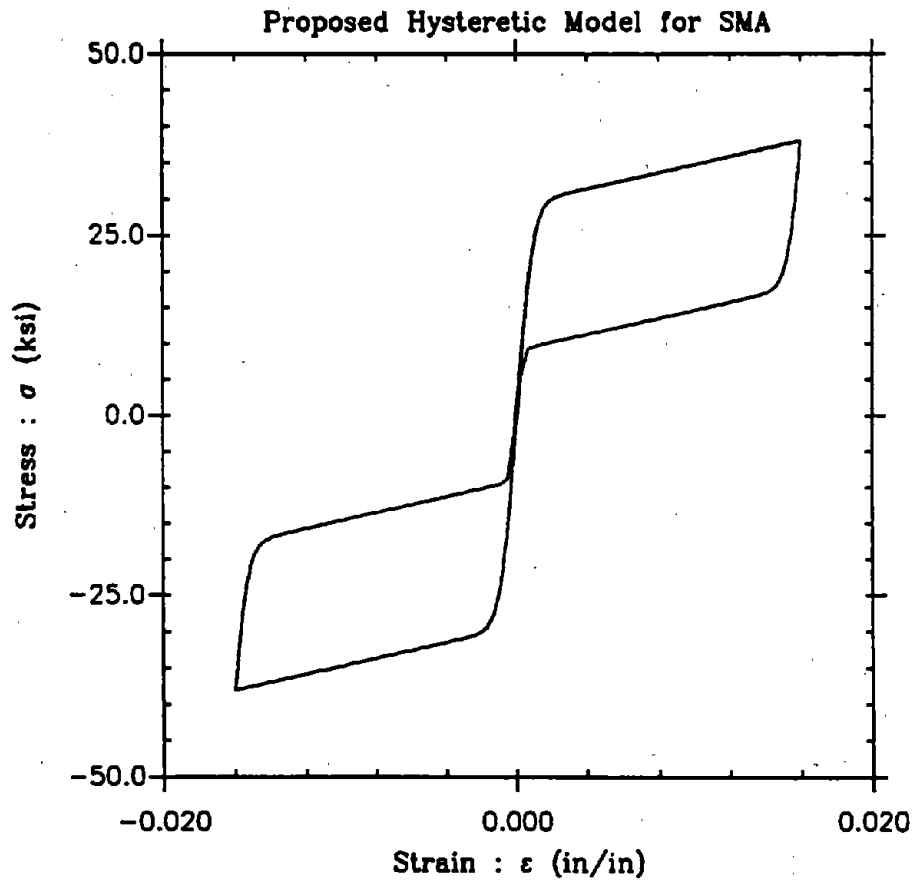
FIGURE 5-10 Cyclic Behavior of SMA with f_T = 0.07; Superelastic Behavior

$\varepsilon = .016 \sin 1^*t$

$Y = 30$ ksi $\nu = 0.5$

$E = 28500$ ksi

$\alpha = 0.0197$

$n = 15$

$a = 3500$ $c = .0005$ $f_\tau = .07$

Proposed Hysteretic Model for SMA
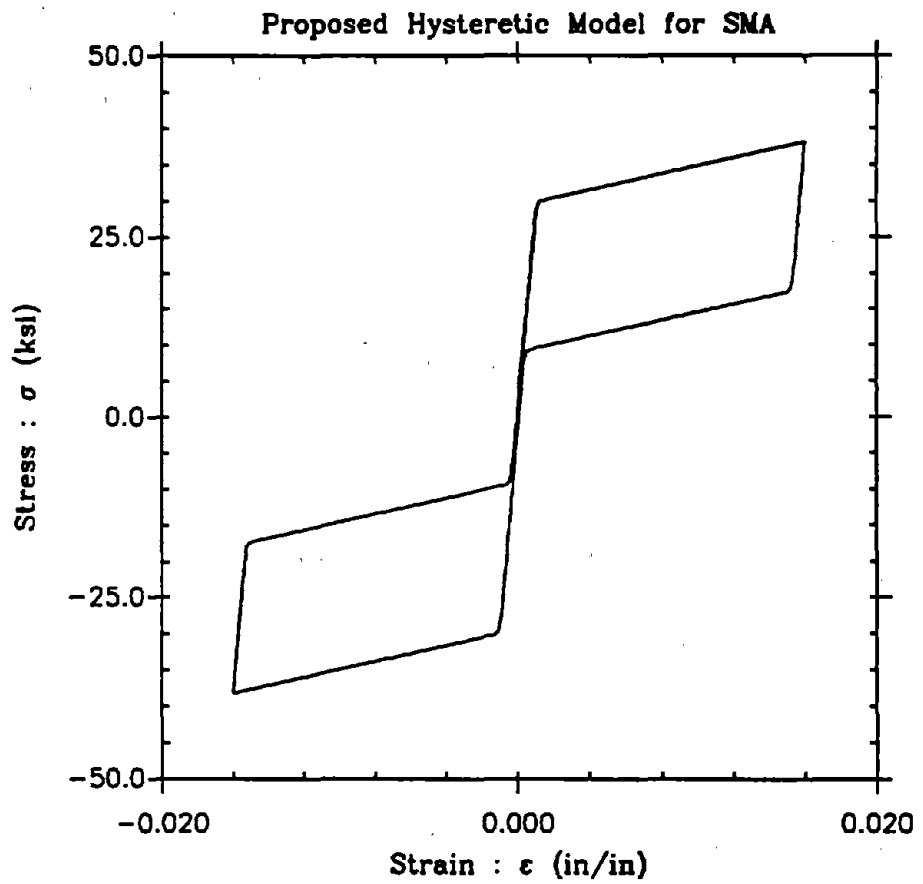
FIGURE 5-11 Superelastic Material Representation with n = 15

$\epsilon = .016 \sin 1^*t$

$Y = 30$ ksi $\quad \nu = 0.5$

$E = 28500$ ksi

$\alpha = 0.0197$

$n = 15$

$a = 3500 \quad c = .0005 \quad f_r = .07$
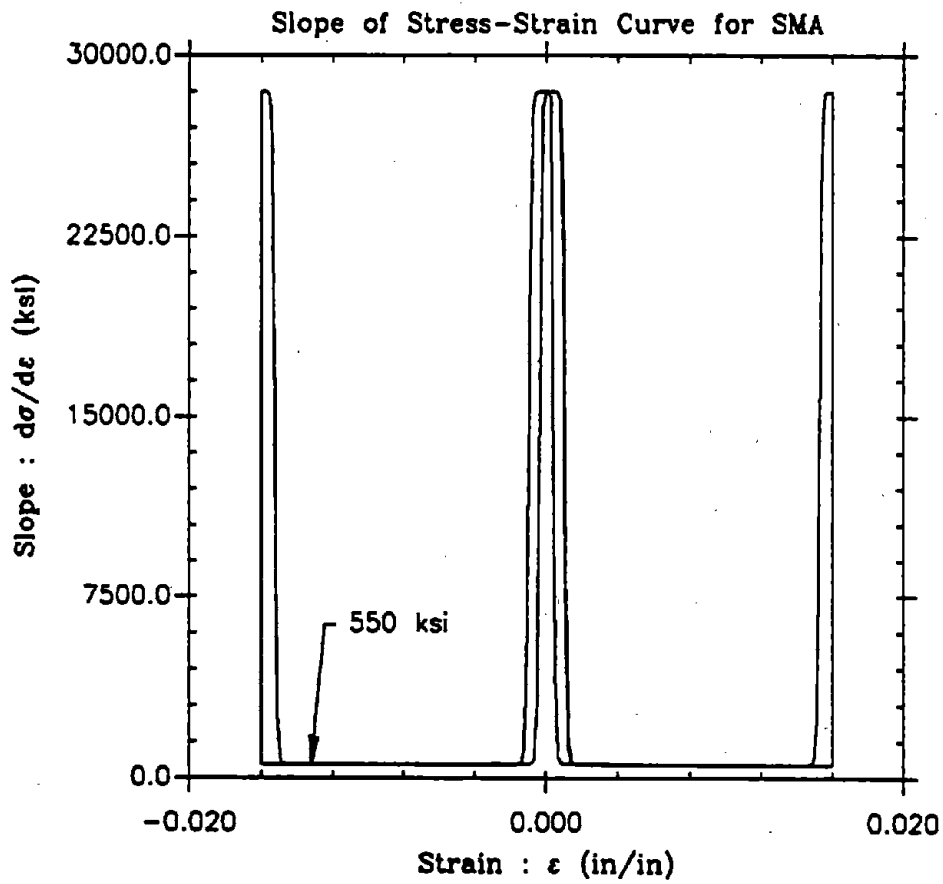
FIGURE 5-12   Slope of Superelastic Hysteresis with n = 15

SECTION 6

CONCLUDING REMARKS

The utilization of Ozdemir's hysteretic model is beneficial from a number of standpoints. The model is relatively simple with respect to many other models of material behavior including models of viscoplasticity. Ozdemir's model contains physically motivated constants in its formulation. Also, the model can be extended to a three-dimensional tensor representation. Furthermore, by modifying the expression for the backstress in Ozdemir's model, a one-dimensional law of shape memory alloy (SMA) behavior is obtained.

By making calculations with the 1D SMA law it is seen that symmetric hysteretic stress-strain curves are able to be generated for low temperature $(T < M_f)$ and superelastic $(T > A_f)$ types of SMA behavior. Also, the physical constants in the model which represent the elastic modulus, initial axial yield, and inelastic modulus are reproduced in the computations. By following a similar methodology to that used in the extension of Ozdemir's model, a three-dimensional tensor representation is proposed for the one-dimensional SMA model.

The computational results presented in this report pertain to one-dimensional uniaxial cyclic material behavior. A number of follow-on projects related to this research have been completed, or are presently in progress. These projects are itemized as follows:

1) Characterization of a Nickel-titanium SMA (Nitinol) in a uniaxial cyclic configuration

2) Determination of SMA model parameters based on the results of Item 1. Evaluation of SMA model capability.

3) Evaluation of the three-dimensional models of metal plasticity and SMA behavior for multi-axial loading conditions.

4) Analysis of the energy absorbing capacity of a plausible SMA energy absorbing device for passive structural damping (either base iaolation or structural bracing). Suggestions for associated experimentation.

SECTION 7

REFERENCES

1. Kelly, J.M., "Aseismic Base Isolation: Review & Bibliography, <u>Soil Dynamics and Earthquake Engineering</u>, Vol. 5, No. 3, 1986, pp. 202-216.

2. Lin, R.C., Liang, Z., Soong, T.T., and Zhang, R.H., "An Experimental Study of Seismic Structural Response with Added.Viscoelastic Dampers," National Center for Earthquake Engineering Research, Technical Report NCEER-88-0018, Buffalo, NY, June 30, 1988.

3. Rath, B.B. and Misra, M.S., "<u>Role of Interfaces on Material Damping</u>," ASM, 1986.

4. Falk, F., "Model Free Energy, Mechanics and Thermodynamics of Shape Memory Alloys," <u>Acta Metallurgica</u>, Vol. 28, pp. 1173-1780.

5   Krishnon, R.V., Delaey, L., Tas, H. and Warlimont, H. "Thermoplasticity, Pseudoelasticity and the Memory Effects Associated with Martinsitic Transformations," <u>Journal of Materials Science</u>, Vol. 4, 1974, pp. 1536-1544.

6. Wen, "Y.K., "Method for Random Vibration of Hysteretic Systems," <u>Journal of Engineering Mechanics Division</u>, ASCE, April, 1986, pp. 249-263.

7. Constantinou, M.C. and Tadjbakhsh, I.G., "Hysteretic Dampers in Base Isolation: Random Approach," <u>Journal of Structural Engineering</u>, ASCE, Vol. iii, No. 4, April, 1985, pp. 705-721.

8. Baber, T.T.,and Noori, M.N., "Random Vibration of Degrading, Pinching Systems," <u>Journal of Engineering Mechanics</u>, ASCE, Vol. iii, No. 8, August, 1985, pp. 1010-1026.

9. Iwan, W.D., "A Distributed-Element Model for Hysteresis and Its Steady-State Dynamic Response," <u>Journal of Applied Mechanics</u>, Trans. ASME, Vol. 8, 1966, pp. 893-400.

10. Miller, A.K., <u>Unified Constitutive Equations for Creep and Plasticity</u>, Elsevier Applied Science, 1987.

11. Krempel, E., "Models of Viscoplasticity Some Comments or Equilibrium (Back) Stress and Drag Stress," <u>Acta Mechanica</u>, Vol. 69, 1987, pp. 25-42.

12. Yao, D., "Theory of Viscoplasticity Based on Overstress with Applications," Ph.D. Dissertation, Rensselaer Polytechnic Institute, Troy, NY, February, 1987.

13. Ozdemir, H., "Nonlinear Transient Dynamic Analysis of Yielding Structures," Ph.D. Dissertation, U.C. Berkeley, Berkeley, CA, June, 1976.

14. Perzyna, P., "Fundamental Problems in Viscoplasticity," <u>Adv. Appl. Mech.</u>, Vol. 9, 1966, pp. 243-377.

15. Achenbach, M., Atanochovic, T. and Muller, I., "A Model for Memory Alloys in Plane Strain," <u>Int. J.Solids Structures</u>, Vol. 22, No. 2, 1986, pp. 171-193.

16. Bhatti, M.A., Pister, K.S. and Polak, E., "Optimal Design of an Earthquake Isolation System," Earthquake Engineering Research Center, Report No. UCB/EERC-78/22, Berkeley, CA, October, 1978.

17. Chang, W.P. and Cozzarelli, F.A., "On the Thermodynamics of Nonlinear Single Integral Representations of Thermoviscoelastic materials with Applications to One-Dimensional Wave Propagation," <u>Acta Mechanica</u>, Vol. 25, 1977, pp. 187-206.

18. Shames, I.H. and Cozzarelli, F.A., <u>Elastic and Inelastic Stress Analysis</u>, to be published by Prentice-Hall Inc., estimated 1990.

19. Abramowitz, M. and Stegun, I.A., ed., <u>Handbook of Mathematical Functions with Formulas, Graphs, and Mathematical Tables</u>, U.S. Dept. of Commerce, June, 1964.

20. Chang, K.C. and Lee, G.C., "Biaxial Properties of Structural Steel Under Nonproportional Loading," _Journal of Engineering Mechanics_, ASCE, Vol. 112, No. 8, August, 1986.
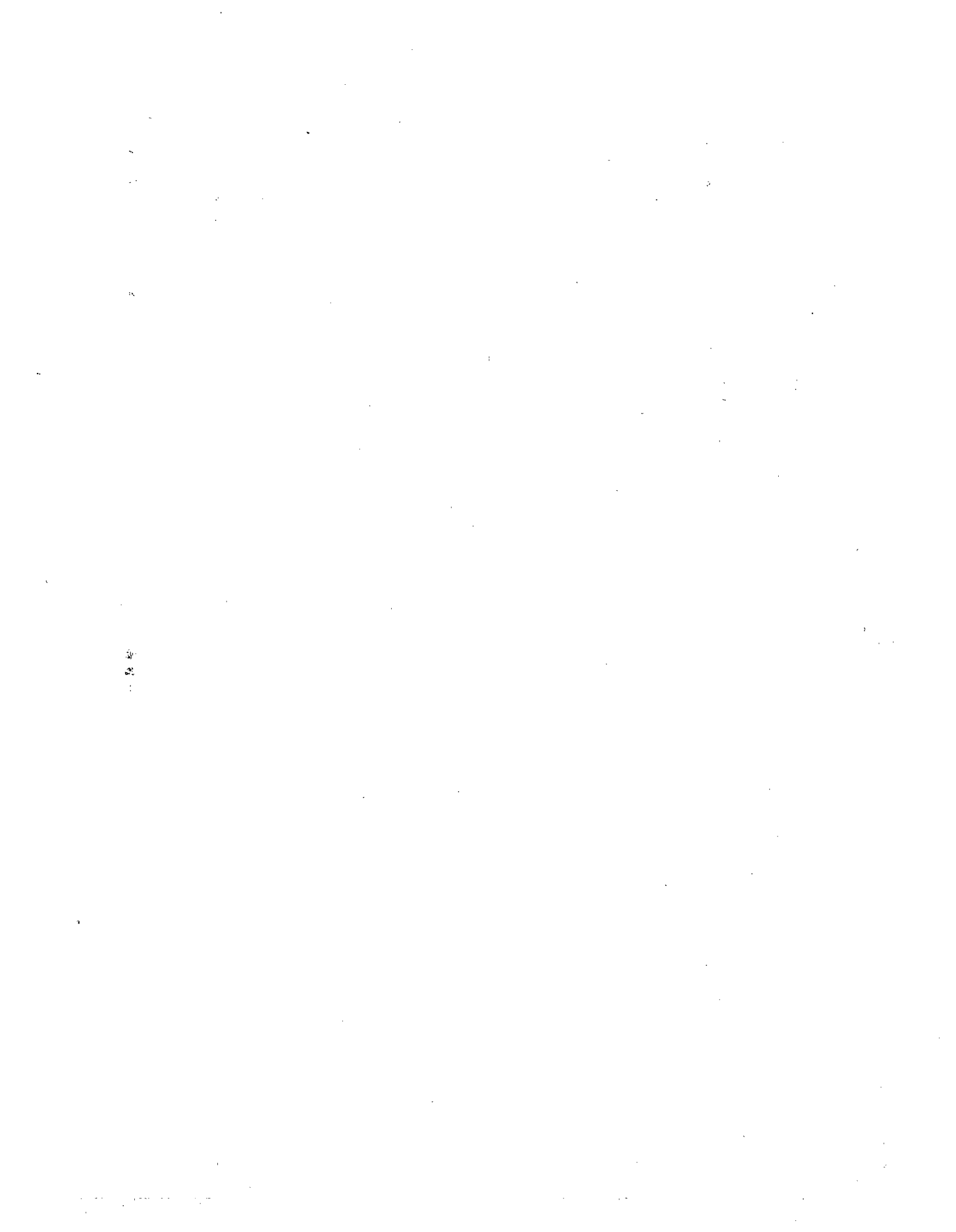
NATIONAL CENTER FOR EARTHQUAKE ENGINEERING RESEARCH
LIST OF PUBLISHED TECHNICAL REPORTS

The National Center for Earthquake Engineering Research (NCEER) publishes technical reports on a variety of subjects related to earthquake engineering written by authors funded through NCEER. These reports are available from both NCEER's Publications Department and the National Technical Information Service (NTIS). Requests for reports should be directed to the Publications Department, National Center for Earthquake Engineering Research, State University of New York at Buffalo, Red Jacket Quadrangle, Buffalo, New York 14261. Reports can also be requested through NTIS, 5285 Port Royal Road, Springfield, Virginia 22161. NTIS accession numbers are shown in parenthesis, if available.

NCEER-87-0001 "First-Year Program in Research, Education and Technology Transfer," 3/5/87, (PB88-134275/AS).

NCEER-87-0002 "Experimental Evaluation of Instantaneous Optimal Algorithms for Structural Control," by R.C. Lin, T.T. Soong and A.M. Reinhorn, 4/20/87, (PB88-134341/AS).

NCEER-87-0003 "Experimentation Using the Earthquake Simulation Facilities at University at Buffalo," by A.M. Reinhorn and R.L. Ketter, to be published.

NCEER-87-0004 "The System Characteristics and Performance of a Shaking Table," by J.S. Hwang, K.C. Chang and G.C. Lee, 6/1/87, (PB88-134259/AS).

NCEER-87-0005 "A Finite Element Formulation for Nonlinear Viscoplastic Material Using a Q Model," by O. Gyebi and G. Dasgupta, 11/2/87, (PB88-213764/AS).

NCEER-87-0006 "Symbolic Manipulation Program (SMP) - Algebraic Codes for Two and Three Dimensional Finite Element Formulations," by X. Lee and G. Dasgupta, 11/9/87, (PB88-219522/AS).

NCEER-87-0007 "Instantaneous Optimal Control Laws for Tall Buildings Under Seismic Excitations," by J.N. Yang, A. Akbarpour and P. Ghaemmaghami, 6/10/87, (PB88-134333/AS).

NCEER-87-0008 "IDARC: Inelastic Damage Analysis of Reinforced Concrete Frame - Shear-Wall Structures," by Y.J. Park, A.M. Reinhorn and S.K. Kunnath, 7/20/87, (PB88-134325/AS).

NCEER-87-0009 "Liquefaction Potential for New York State: A Preliminary Report on Sites in Manhattan and Buffalo," by M. Budhu, V. Vijayakumar, R.F. Giese and L. Baumgras, 8/31/87, (PB88-163704/AS). This report is available only through NTIS (see address given above).

NCEER-87-0010 "Vertical and Torsional Vibration of Foundations in Inhomogeneous Media," by A.S. Veletsos and K.W. Dotson, 6/1/87, (PB88-134291/AS).

NCEER-87-0011 "Seismic Probabilistic Risk Assessment and Seismic Margins Studies for Nuclear Power Plants," by Howard H.M. Hwang, 6/15/87, (PB88-134267/AS). This report is available only through NTIS (see address given above).

NCEER-87-0012 "Parametric Studies of Frequency Response of Secondary Systems Under Ground-Acceleration Excitations," by Y. Yong and Y.K. Lin, 6/10/87, (PB88-134309/AS).

NCEER-87-0013 "Frequency Response of Secondary Systems Under Seismic Excitation," by J.A. HoLung, J. Cai and Y.K. Lin, 7/31/87, (PB88-134317/AS).

NCEER-87-0014 "Modelling Earthquake Ground Motions in Seismically Active Regions Using Parametric Time Series Methods," by G.W. Ellis and A.S. Cakmak, 8/25/87, (PB88-134283/AS).

NCEER-87-0015 "Detection and Assessment of Seismic Structural Damage," by E. DiPasquale and A.S. Cakmak, 8/25/87, (PB88-163712/AS).

NCEER-87-0016 "Pipeline Experiment at Parkfield, California," by J. Isenberg and E. Richardson, 9/15/87, (PB88-163720/AS).

NCEER-87-0017   "Digital Simulation of Seismic Ground Motion," by M. Shinozuka, G. Deodatis and T. Harada, 8/31/87, (PB88-155197/AS). This report is available only through NTIS (see address given above).

NCEER-87-0018   "Practical Considerations for Structural Control: System Uncertainty, System Time Delay and Truncation of Small Control Forces," J.N. Yang and A. Akbarpour, 8/10/87, (PB88-163738/AS).

NCEER-87-0019   "Modal Analysis of Nonclassically Damped Structural Systems Using Canonical Transformation," by J.N. Yang, S. Sarkani and F.X. Long, 9/27/87, (PB88-187851/AS).

NCEER-87-0020   "A Nonstationary Solution in Random Vibration Theory," by J.R. Red-Horse and P.D. Spanos, 11/3/87, (PB88-163746/AS).

NCEER-87-0021   "Horizontal Impedances for Radially Inhomogeneous Viscoelastic Soil Layers," by A.S. Veletsos and K.W. Dotson, 10/15/87, (PB88-150859/AS).

NCEER-87-0022   "Seismic Damage Assessment of Reinforced Concrete Members," by Y.S. Chung, C. Meyer and M. Shinozuka, 10/9/87, (PB88-150867/AS). This report is available only through NTIS (see address given above).

NCEER-87-0023   "Active Structural Control in Civil Engineering," by T.T. Soong, 11/11/87, (PB88-187778/AS).

NCEER-87-0024   Vertical and Torsional Impedances for Radially Inhomogeneous Viscoelastic Soil Layers," by K.W. Dotson and A.S. Veletsos, 12/87, (PB88-187786/AS).

NCEER-87-0025   "Proceedings from the Symposium on Seismic Hazards, Ground Motions, Soil-Liquefaction and Engineering Practice in Eastern North America," October 20-22, 1987, edited by K.H. Jacob, 12/87, (PB88-188115/AS).

NCEER-87-0026   "Report on the Whittier-Narrows, California, Earthquake of October 1, 1987," by J. Pantelic and A. Reinhorn, 11/87, (PB88-187752/AS). This report is available only through NTIS (see address given above).

NCEER-87-0027   "Design of a Modular Program for Transient Nonlinear Analysis of Large 3-D Building Structures," by S. Srivastav and J.F. Abel, 12/30/87, (PB88-187950/AS).

NCEER-87-0028   "Second-Year Program in Research, Education and Technology Transfer," 3/8/88, (PB88-219480/AS).

NCEER-88-0001   "Workshop on Seismic Computer Analysis and Design of Buildings With Interactive Graphics," by W. McGuire, J.F. Abel and C.H. Conley, 1/18/88, (PB88-187760/AS).

NCEER-88-0002   "Optimal Control of Nonlinear Flexible Structures," by J.N. Yang, F.X. Long and D. Wong, 1/22/88, (PB88-213772/AS).

NCEER-88-0003   "Substructuring Techniques in the Time Domain for Primary-Secondary Structural Systems," by G.D. Manolis and G. Juhn, 2/10/88, (PB88-213780/AS).

NCEER-88-0004   "Iterative Seismic Analysis of Primary-Secondary Systems," by A. Singhal, L.D. Lutes and P.D. Spanos, 2/23/88, (PB88-213798/AS).

NCEER-88-0005   "Stochastic Finite Element Expansion for Random Media," by P.D. Spanos and R. Ghanem, 3/14/88, (PB88-213806/AS).

NCEER-88-0006   "Combining Structural Optimization and Structural Control," by F.Y. Cheng and C.P. Pantelides, 1/10/88, (PB88-213814/AS).

NCEER-88-0007   "Seismic Performance Assessment of Code-Designed Structures," by H.H-M. Hwang, J-W. Jaw and H-J. Shau, 3/20/88, (PB88-219423/AS).

NCEER-88-0008   "Reliability Analysis of Code-Designed Structures Under Natural Hazards," by H.H-M. Hwang, H. Ushiba and M. Shinozuka, 2/29/88, (PB88-229471/AS).

NCEER-88-0009   "Seismic Fragility Analysis of Shear Wall Structures," by J-W Jaw and H.H-M. Hwang, 4/30/88, (PB89-102867/AS).

NCEER-88-0010   "Base Isolation of a Multi-Story Building Under a Harmonic Ground Motion - A Comparison of Performances of Various Systems," by F-G Fan, G. Ahmadi and I.G. Tadjbakhsh, 5/18/88, (PB89-122238/AS).

NCEER-88-0011   "Seismic Floor Response Spectra for a Combined System by Green's Functions," by F.M. Lavelle, L.A. Bergman and P.D. Spanos, 5/1/88, (PB89-102875/AS).

NCEER-88-0012   "A New Solution Technique for Randomly Excited Hysteretic Structures," by G.Q. Cai and Y.K. Lin, 5/16/88, (PB89-102883/AS).

NCEER-88-0013   "A Study of Radiation Damping and Soil-Structure Interaction Effects in the Centrifuge," by K. Weissman, supervised by J.H. Prevost, 5/24/88, (PB89-144703/AS).

NCEER-88-0014   "Parameter Identification and Implementation of a Kinematic Plasticity Model for Frictional Soils," by J.H. Prevost and D.V. Griffiths, to be published.

NCEER-88-0015   "Two- and Three- Dimensional Dynamic Finite Element Analyses of the Long Valley Dam," by D.V. Griffiths and J.H. Prevost, 6/17/88, (PB89-144711/AS).

NCEER-88-0016   "Damage Assessment of Reinforced Concrete Structures in Eastern United States," by A.M. Reinhorn, M.J. Seidel, S.K. Kunnath and Y.J. Park, 6/15/88, (PB89-122220/AS).

NCEER-88-0017   "Dynamic Compliance of Vertically Loaded Strip Foundations in Multilayered Viscoelastic Soils," by S. Ahmad and A.S.M. Israil, 6/17/88, (PB89-102891/AS).

NCEER-88-0018   "An Experimental Study of Seismic Structural Response With Added Viscoelastic Dampers," by R.C. Lin, Z. Liang, T.T. Soong and R.H. Zhang, 6/30/88, (PB89-122212/AS).

NCEER-88-0019   "Experimental Investigation of Primary - Secondary System Interaction," by G.D. Manolis, G. Juhn and A.M. Reinhorn, 5/27/88, (PB89-122204/AS).

NCEER-88-0020   "A Response Spectrum Approach For Analysis of Nonclassically Damped Structures," by J.N. Yang, S. Sarkani and F.X. Long, 4/22/88, (PB89-102909/AS).

NCEER-88-0021   "Seismic Interaction of Structures and Soils: Stochastic Approach," by A.S. Veletsos and A.M. Prasad, 7/21/88, (PB89-122196/AS).

NCEER-88-0022   "Identification of the Serviceability Limit State and Detection of Seismic Structural Damage," by E. DiPasquale and A.S. Cakmak, 6/15/88, (PB89-122188/AS).

NCEER-88-0023   "Multi-Hazard Risk Analysis: Case of a Simple Offshore Structure," by B.K. Bhartia and E.H. Vanmarcke, 7/21/88, (PB89-145213/AS).

NCEER-88-0024   "Automated Seismic Design of Reinforced Concrete Buildings," by Y.S. Chung, C. Meyer and M. Shinozuka, 7/5/88, (PB89-122170/AS).

NCEER-88-0025   "Experimental Study of Active Control of MDOF Structures Under Seismic Excitations," by L.L. Chung, R.C. Lin, T.T. Soong and A.M. Reinhorn, 7/10/88, (PB89-122600/AS).

NCEER-88-0026   "Earthquake Simulation Tests of a Low-Rise Metal Structure," by J.S. Hwang, K.C. Chang, G.C. Lee and R.L. Ketter, 8/1/88, (PB89-102917/AS).

NCEER-88-0027   "Systems Study of Urban Response and Reconstruction Due to Catastrophic Earthquakes," by F. Kozin and H.K. Zhou, 9/22/88, to be published.

NCEER-88-0028　　　"Seismic Fragility Analysis of Plane Frame Structures," by H.H.-M. Hwang and Y.K. Low, 7/31/88, (PB89-131445/AS).

NCEER-88-0029　　　"Response Analysis of Stochastic Structures," by A. Kardara, C. Bucher and M. Shinozuka, 9/22/88, (PB89-174429/AS).

NCEER-88-0030　　　"Nonnormal Accelerations Due to Yielding in a Primary Structure," by D.C.K. Chen and L.D. Lutes, 9/19/88, (PB89-131437/AS).

NCEER-88-0031　　　"Design Approaches for Soil-Structure Interaction," by A.S. Veletsos, A.M. Prasad and Y. Tang, 12/30/88, (PB89-174437/AS).

NCEER-88-0032　　　"A Re-evaluation of Design Spectra for Seismic Damage Control," by C.J. Turkstra and A.G. Tallin, 11/7/88, (PB89-145221/AS).

NCEER-88-0033　　　"The Behavior and Design of Noncontact Lap Splices Subjected to Repeated Inelastic Tensile Loading," by V.E. Sagan, P. Gergely and R.N. White, 12/8/88.

NCEER-88-0034　　　"Seismic Response of Pile Foundations," by S.M. Mamoon, P.K. Banerjee and S. Ahmad, 11/1/88, (PB89-145239/AS).

NCEER-88-0035　　　"Modeling of R/C Building Structures With Flexible Floor Diaphragms (IDARC2)," by A.M. Reinhorn, S.K. Kunnath and N. Panahshahi, 9/7/88, (PB89-207153/AS).

NCEER-88-0036　　　"Solution of the Dam-Reservoir Interaction Problem Using a Combination of FEM, BEM with Particular Integrals, Modal Analysis, and Substructuring," by C-S. Tsai, G.C. Lee and R.L. Ketter, 12/31/88, (PB89-207146/AS).

NCEER-88-0037　　　"Optimal Placement of Actuators for Structural Control," by F.Y. Cheng and C.P. Pantelides, 8/15/88.

NCEER-88-0038　　　"Teflon Bearings in Aseismic Base Isolation: Experimental Studies and Mathematical Modeling," by A. Mokha, M.C. Constantinou and A.M. Reinhorn, 12/5/88.

NCEER-88-0039　　　"Seismic Behavior of Flat Slab High-Rise Buildings in the New York City Area," by P. Weidlinger and M. Ettouney, 10/15/88, to be published.

NCEER-88-0040　　　"Evaluation of the Earthquake Resistance of Existing Buildings in New York City," by P. Weidlinger and M. Ettouney, 10/15/88, to be published.

NCEER-88-0041　　　"Small-Scale Modeling Techniques for Reinforced Concrete Structures Subjected to Seismic Loads," by W. Kim, A. El-Attar and R.N. White, 11/22/88, (PB89-189625/AS).

NCEER-88-0042　　　"Modeling Strong Ground Motion from Multiple Event Earthquakes," by G.W. Ellis and A.S. Cakmak, 10/15/88, (PB89-174445/AS).

NCEER-88-0043　　　"Nonstationary Models of Seismic Ground Acceleration," by M. Grigoriu, S.E. Ruiz and E. Rosenblueth, 7/15/88, (PB89-189617/AS).

NCEER-88-0044　　　"SARCF User's Guide: Seismic Analysis of Reinforced Concrete Frames," by Y.S. Chung, C. Meyer and M. Shinozuka, 11/9/88, (PB89-174452/AS).

NCEER-88-0045　　　"First Expert Panel Meeting on Disaster Research and Planning," edited by J. Pantelic and J. Stoyle, 9/15/88, (PB89-174460/AS).

NCEER-88-0046　　　"Preliminary Studies of the Effect of Degrading Infill Walls on the Nonlinear Seismic Response of Steel Frames," by C.Z. Chrysostomou, P. Gergely and J.F. Abel, 12/19/88, (PB89-208383/AS).

NCEER-88-0047　　　"Reinforced Concrete Frame Component Testing Facility - Design, Construction, Instrumentation and Operation," by S.P. Pessiki, C. Conley, T. Bond, P. Gergely and R.N. White, 12/16/88, (PB89-174478/AS).

A-4

NCEER-89-0001   "Effects of Protective Cushion and Soil Compliancy on the Response of Equipment Within a Seismically Excited Building," by J.A. HoLung, 2/16/89, (PB89-207179/AS).

NCEER-89-0002   "Statistical Evaluation of Response Modification Factors for Reinforced Concrete Structures," by H.H-M. Hwang and J-W. Jaw, 2/17/89, (PB89-207187/AS).

NCEER-89-0003   "Hysteretic Columns Under Random Excitation," by G-Q. Cai and Y.K. Lin, 1/9/89, (PB89-196513/AS).

NCEER-89-0004   "Experimental Study of 'Elephant Foot Bulge' Instability of Thin-Walled Metal Tanks," by Z-H. Jia and R.L. Ketter, 2/22/89, (PB89-207195/AS).

NCEER-89-0005   "Experiment on Performance of Buried Pipelines Across San Andreas Fault," by J. Isenberg, E. Richardson and T.D. O'Rourke, 3/10/89.

NCEER-89-0006   "A Knowledge-Based Approach to Structural Design of Earthquake-Resistant Buildings," by M. Subramani, P. Gergely, C.H. Conley, J.F. Abel and A.H. Zaghw, 1/15/89.

NCEER-89-0007   "Liquefaction Hazards and Their Effects on Buried Pipelines," by T.D. O'Rourke and P.A. Lane, 2/1/89.

NCEER-89-0008   "Fundamentals of System Identification in Structural Dynamics," by H. Imai, C-B. Yun, O. Maruyama and M. Shinozuka, 1/26/89, (PB89-207211/AS).

NCEER-89-0009   "Effects of the 1985 Michoacan Earthquake on Water Systems and Other Buried Lifelines in Mexico," by A.G. Ayala and M.J. O'Rourke, 3/8/89, (PB89-207229/AS).

NCEER-89-0010   "NCEER Bibliography of Earthquake Education Materials," by K.E.K. Ross, 3/10/89.

NCEER-89-0011   "Inelastic Three-Dimensional Response Analysis of Reinforced Concrete Building Structures (IDARC-3D), Part I - Modeling," by S.K. Kunnath and A.M. Reinhorn, 4/17/89.

NCEER-89-0012   "Recommended Modifications to ATC-14," by C.D. Poland and J.O. Malley, 4/12/89.

NCEER-89-0013   "Repair and Strengthening of Beam-to-Column Connections Subjected to Earthquake Loading," by M. Corazao and A.J. Durrani, 2/28/89.

NCEER-89-0014   "Program EXKAL2 for Identification of Structural Dynamic Systems," by O. Maruyama, C-B. Yun, M. Hoshiya and M. Shinozuka, 5/19/89.

NCEER-89-0015   "Response of Frames With Bolted Semi-Rigid Connections, Part I - Experimental Study and Analytical Predictions," by P.J. DiCorso, A.M. Reinhorn, J.R. Dickerson, J.B. Radziminski and W.L. Harper, 6/1/89, to be published.

NCEER-89-0016   "ARMA Monte Carlo Simulation in Probabilistic Structural Analysis," by P.D. Spanos and M.P. Mignolet, 7/10/89.

NCEER-89-0017   "Preliminary Proceedings of the Conference on Disaster Preparedness - The Place of Earthquake Education in Our Schools, July 9-11, 1989," 6/23/89.

NCEER-89-0018   "Multidimensional Models of Hysteretic Material Behavior for Vibration Analysis of Shape Memory Energy Absorbing Devices, by E.J. Graesser and F.A. Cozzarelli, 6/7/89.